DEUTSCHES ELEKTRONEN – SYNCHROTRON DESY

DESY 89-023
February 1989

Fast Ground Motion at HERA

J. Rossbach
Deutsches Elektronen-Synchrotron DESY, Hamburg

ISSN 0418-9833

NOTKESTRASSE 85 · 2 HAMBURG 52

DESY 89- 023 *
February 1989

ISSN 0418-9833

Fast Ground Motion at HERA

J. Rossbach
Deutsches Elektronen-Synchrotron DESY Hamburg

* Instead of the Report DESY HERA 87-17 (1987) which has not been printed.

ABSTRACT

A number of measurements and theoretical considerations have been performed to estimate the electron-proton beam separation in HERA due to fast ground motion. Typical ground motion amplitudes of 0.2 μm have been found, but the quadrupole magnet motion is larger by a factor of 2-5 due to resonances of the supports. The resulting closed orbit distortion has been investigated analytically as well as numerically. The effect of ground waves instead of uncorrelated quadrupole motion has been considered. The estimated horizontal as well as vertical beam separation is of the order of one tenth of the respective beam sizes.

1. INTRODUCTION

Ground motion occurs in a wide range of amplitudes and frequencies. Its spectrum varies considerably with time and sites under consideration. For our purpose, namely the impact on closed orbit stability in HERA, we may neglect extraordinarily rare events like earthquakes, heavy storms, blasting operation nearby, etc., since these will not injure the overall performance of HERA. We will not consider either very slow ground motion (time constants longer than approx. 10 min.) although its amplitude may be very large. This motion can be detected and compensated by survey and realignment procedures and/or orbit correction methods.

As far as fast ground motion is concerned, we shall *assume* in this report that it occurs only as weakly damped ground waves. This plausible but unproven assumption will be subject of further investigations. If it is valid, frequencies below approx. 1 Hz will not play any role, because they correspond to ground wave lengths larger than the HERA diameter $2R \approx 2$ km[1,2]. If it were not, one had to measure ground motion frequencies below 1 Hz on a submicrometer level, which requires considerable experimental effort.

In the past, closed orbit distortions due to ground motion have been of minor importance for storage rings, since either

a) beam sizes of colliding beams have been several orders of magnitude larger than ground motion amplitudes (millimeters as compared to micrometers, see e.g. ISR and DORIS)

or

b) storage rings have been operated as single ring colliding beams facilities (SPS, PETRA, TEVATRON, PEP, ...)

In the latter case, it is guaranteed by first principles, that particles and antiparticles join the same closed orbit and collide centrically, because they share the same magnetic guiding fields.

With HERA, however, beam sizes are in the μm range (beam heights at the interaction points below approx. 70 μm), and the colliding beams are stored in two very different magnet lattices, which, although installed in the same tunnel, respond to ground motion in considerably different ways. In addition, the amplitude of closed orbit distortions due to ground motion is expected to scale stronger than linearly with the ring size.. This is, because the closed orbit response to ground motion increases with the number of quadrupole magnets involved, and because increasing ring size means lower ground noise frequency components to become more relevant, which in turn are known to have larger amplitudes (see e.g. ref. 3 and fig. 1.2 in ref. 4). As a consequence, fast ground motion might be an important item for HERA and requires careful investigation of ground motion as well as magnet motion and closed orbit response.

2. INSTRUMENTATION

The aim was measurement of fast ground motion ($\nu \geq 1$ Hz) with precision $\lesssim 0.1 \mu m$ at different positions on the HERA perimeter as a function of time of day. Long term measurements (to find peak values) were desired as well as averaging and spectrum analysis. The equipment had to be transportable and easy to install. During a first period of measurements, the portable seismometer model 18 300 of Teledyne Geotech, USA, has been used, see fig. 1. It is available in two versions for horizontal or vertical measurement, respectively. It consists of a 5 kg inertial mass suspended from 3 stiff springs. The resonance frequency of this mechanical oscillator is about 1 Hz. The motion of the mass with respect to the support is transformed into an electrical voltage by an induction coil (fixed on the mass) moving in a magnetic field. It is externally loaded by a resistor in order to obtain optimum damping for the best flat response to velocity (approx. $\sqrt{2}$ times the critical damping resistance). Thus, for $\nu > 1$ Hz the output voltage is proportional to the ground velocity. To obtain displacement signals, the output has been integrated once on line. The circuitry is sketched in fig. 2.

From calibration constants as provided by the manufacturer and from parameters of the external circuitry a gauge (μm displacement per Volt output) can be derived. As an independent check, the setup has been calibrated at a large scale seismometer of the Geophysics Institute of the Hamburg University (outpost Harburg), see fig. 3. It is seen that the agreement is better than 10 % for frequencies ≥ 1 Hz. The marked 0.25 Hz component, however, which presumably stems from sea waves, is present in the large seismometer's signal only.

For measurements on the floor, the portable seismometer is perfect. With respect to closed orbit distortions, however, motion of the magnetic quadrupole fields is more relevant. Much smaller and lighter probes are required for measurements on or inside magnets. Acceleration probes type 4379 by Brüel & Kjaer, Denmark, have proven useful. The diameter is 44 mm and the weight 175 g only. Nevertheless, the precision is much better than 1 μm for frequencies above 1 Hz. Since the piezoelectric effect is used, the probe's signal is proportional to its acceleration. Therefore, the precision with respect to displacement becomes better in proportion to the square of the frequency. A suitable preamplifier performs double integration. For long term measurements of ground velocity and displacement versus real time an analog paper strip recorder has been used. It was well-suited for detection of extraordinary events and variance analysis, but time resolution was bad. Thus, for short term (e.g. 10 sec) recording a Hewlett Packard digital plotter has been preferred. In addition to time domain representation, signals have have been Fourier transformed by a spectrum analyser. Most spectra have been averaged for about 10 minutes, until fluctuations did not affect the spectrum any more. In order to analyse short term behaviour, however, fast Fourier transforms of short periods as well as time domain representation have been more useful, of course. In any case, the "flat top" filter of the spectrum analyser has been used, which guarantees optimum amplitude precision.

Future plans include digital signal processing and storage as well as correlation analysis. Special attention will be paid to the motion of superconducting quadrupole magnets and slow drifts of the interaction regions.

3. GROUND MOTION

It is known from experience that in industrialized regions the high frequency (≥ 1 Hz) part of the ground motion is dominated by man made noise[3,4]. As seen from fig. 4, HERA approaches on its course a number of different kinds of sources. E.g. there is a railroad line in the north-east,a highway in the east, several industrial plants like a refuse incineration plant and DESY itself, and there is a main road (Luruper Hauptstraße) crossing twice. Data have been take at four positions on the perimeter, namely at both of the main road crossings and at two positions where no source nearby is known. These points are marked 1, 2, 3 in fig. 4, respectively. For comparison a number of measurements have been taken at different points on the DESY ground (not reported here). The result was, that there is no significant difference between ground surface motion and motion of the HERA tunnel which is about 10 - 20 m below ground.

Fig. 5 shows the vertical motion on the HERA tunnel floor at point 2 over a period of 80 sec during working hours, i.e. there was lots of traffic on the Luruper Hauptstraße. The average amplitude is about 0.3 μm including few events of approx. 5 sec duration with amplitudes of up to 0.7 μm. A period of 5 sec is shown in fig. 6 with better time resolution. A 10 minute average spectrum is plotted in fig. 7. As perceptible from the time domain representations already, there is clearly a peak between 2 Hz and 5 Hz. Using a typical phase velocity of Rayleigh waves in the molasse of 2 km/s[3], this corresponds to wavelengths λ between 400 m and 1000 m or $2\pi R/\lambda = C/\lambda$ between 6 and 16. It is seen from ref. 2 and section 5 of the present report, that these C/λ values are below the critical ones for HERA - but not far below. Thus, verification of the phase velocity assumption is of particular interest. Fig. 7 is complemented by fig. 8, a "map" representation of 30 fast Fourier transformations. The 50 Hz component in the spectra might be due to stray fields. Data from point 3 (no exceptional source nearby) are shown in fig. 9. Obviously the vertical noise level is significantly lower than at points 1 and 2. This statement is *not* valid for the horizontal motion, which is evidently the same at all points 1, 2, 3, 4. It is shown for point 3 in figs. 10 and 11, and fig. 12 shows an averaged spectrum from point 1. As indicated on each plot, most of the data shown have been taken during working hours. A number of measurements have been performed between 8pm and 9pm. The result was that the "steady" level of horizontal and vertical ground noise was nearly unchanged, but extraordinary events are much more sporadic. Table 1 compiles results from ground motion measurements on the HERA tunnel floor.

4. MOTION OF MAGNETS

What really matters with respect to closed orbit distortions is not ground motion but motion of quadrupole magnets. This can be considerably different due to the elastic behaviour of the magnet's supports.

a) Electron ring

Measurement of the motion of the *electron* ring quadrupole magnets was fairly easy. They are of conventional, normal conducting type and they are mounted on a rigid girder, in common with sextupole magnets and bending magnet endings (see fig. 13). The seismometer was placed either on the girder close to the quadrupole or on top of the quadrupole, which results in considerably different motion spectra, see figs. 14-16. The difference is due to two vertical eigenmodes of the dipole magnet at 4.5 Hz and 6.2 Hz. Since the girder is supported at the center of the quadrupole, these modes are very effectively suppressed for the quadrupole motion, but become more and more dominant with increasing distance from the quadrupole center. Peak to peak amplitudes of 4 μm are typical for the vertical motion of the electron dipole magnets, see fig. 17.

For closed orbit distortions, however, only the quadrupole motion matters, and we can keep in mind from figs. 15, 16, that the vertical rms motion of the quadrupole magnets is amplified by a factor of about 1.5 ... 2.0 as compared to the ground motion.

Table 1: Summary of measurements.
The rms-*amplitude* $\sigma_A = \sqrt{2}\sqrt{< x^2 >}$ is given.

Horizontal

$\sigma_A = (0.2 \pm 0.05)\ \mu m$ $\quad \nu \geq 3$ Hz
sometimes 0.4 μm at $\nu = 1 \dots 2$ Hz
below main road not significantly more than 140 m aside

Vertical

	during working hours	> 8pm
below main road	$(0.3 \pm 0.1)\ \mu m$ ≥ 50 % of which within $3 < \nu < 5\ Hz$ ≈ 2/min amplitudes $\approx 0.7\ \mu m$, 5 sec long	$(0.25 \pm 0.05)\ \mu m$ $\nu \geq 3$ Hz
140 m aside	$(0.15 \pm 0.05)\ \mu m$ ≥ 50 % within $3 < \nu < 5\ Hz$	
Hamburg geophysics institute: few industry and traffic except: 300 m from highway	$(0.2 \pm 0.05)\ \mu m$ ≥ 50 % within $3 < \nu < 5\ Hz$	

This is the result from measurements in the periodic arc (point 3 in fig. 4), but quadrupole supports are considerably different in the straight sections, and there are different types of supports in the straight sections. The worst case (as far as the electron ring is concerned) has been found on position 197 m left from Hall North (see point 4 in fig. 4). A typical 5 seconds periods of the vertical motion is shown in fig. 18, and fig. 19 shows the corresponding spectrum. The motion is characterized by an eigenmode at 7 Hz and its 3rd harmonic. Actually, this mode is a horizontal one, which shows up from fig. 20. The quadrupole is mounted on a cantilever arm at this position. At most other positions this

kind of motion is damped by a horizontal iron prop. This yields a horizontal quadrupole motion as shown in fig. 21, which is much smaller but still approx. 4 times larger that the ground motion (see fig. 11). This factor 4 as well describes the horizontal motion of the electron quadrupole magnets in the arc.
Summary of the electron quadrupole motion measurements is as follows. The vertical rms motion is approx. 2 times, and the average horizontal motion approx. 5 times larger than the respective ground motion. Whether or not the motion of neighbouring quadrupoles is correlated (for example in accordance with ground waves moving along) is unknown and remains to be measured. Magnet cooling water was off during all measurements.

b) Proton ring

Detection of the quadrupole motion in the HERA proton ring is much more complicated as compared to the electron ring, because proton quadrupoles are cold bore superconducting magnets. Only very preliminary results are reported here indicating that there is a considerable amplification of ground motion. The reason is, that for heat insulation reasons there cannot be a rigid connection between the superconducting coil and the warm part of the cryostat tank. Instead, the superconducting coil (including iron yoke and beam pipe) is suspended quite loosely from the outer vacuum vessel. Figs. 22-24 show the motion of the proton quadrupole cryostat as measured on top of the outer tank, with the whole cryostat mounted on its final supports in the HERA tunnel (position 1 in fig. 4), but without any helium flowing, i.e. with the magnet at room temperature. As stated already, it is the motion of the magnetic field what matters and not the motion of the cryostat and, moreover, real operation conditions will be different. But, nevertheless, these measurements show that there are some high Q mechanical modes of the cryostat system. Using the Brüel & Kjaer acceleration probe, the motion inside the vacuum pipe has been measured (note that the vacuum pipe is an integral part of the superconducting magnet). The result of this room temperature measurement is reported in figs. 25-27. The preliminary result is an amplification factor of approx. 2 and max. 4 for the vertical and horizontal proton quadrupole motion, respectively. Measurements under much more realistic conditions are in preparation.

5. MODELLING OF THE CLOSED-ORBIT RESPONSE

a) Analytical Model

If the effect of nonlinear elements like sextupole magnets is neglected, the closed orbit distortion due to any quadrupole misalignment can be calculated analytically. If many quadrupole magnets are involved, however, the result will be extremely complicated and in general it will be hard to draw conclusions. If the misalignments are due to horizontal or vertical plane ground waves, one could think of rearranging the complicated sum into a more instructive form, which more clearly exhibits the resonance-like closed orbit response whenever the ground wavelength λ equals some spacial periodicity of the linear optics. This has been done for a ring with continuous focusing inf ref. 1 and for a model periodic FODO lattice in ref. 2.

It is seen that the closed orbit response R, i.e. the amplitude of the closed orbit distortion at a given position on the ring perimeter, divided by the amplitude of the ground wave, can be expressed as

$$R = \sqrt{\sum_{p=0}^{\infty} C_p \,(\text{optics}, \theta_o) \cdot J_p^2\,(\frac{C}{\lambda})} \qquad (1)$$

J_p are Bessel functions of the first kind and C is the storage ring circumference. The coefficients C_p depend on optical lattice parameters and on the wave direction θ_o. They behave resonantly whenever

$$p = mN \pm Q \qquad (2)$$

N is the number of FODO cells in the ring, Q is the betatron tune (horizontal or vertical Q for horizontal or vertical waves, respectively), and m is an integer. From this formula one expects, with increasing C/λ, the closed orbit response to increase in a step-like manner whenever C/λ exceeds some value

$$Q,\ N-Q,\ N+Q,\ 2N-Q,\ 2N+Q,\ \ldots$$

The formalism becomes much more valuable due to the fact that the result remains nearly unchanged if an ensemble of uncorrelated plane waves with arbitrary phases, amplitudes, and directions is considered. In this case, the coefficients C_p don't depend on wave parameters any more and the resonance condition (2) remains unchanged. The response function is in that case a rms response, of course. For modelling the HERA lattice, N = 130 has been used for the proton ring and N = 280 for the electron ring. Figs. 28 and 29 show the response functions as a function of C/λ for the electron and proton ring, respectively. The response is scaled for an amplitude function $\beta = 1\ m$ at the point of observation. In each plot, the upper curve corresponds to the single wave response and the lower one to the rms response. In addition, the rms response to uncorrelated quadrupole motion is plotted for comparison (broken straight line). All horizontal waves have been assumed to be of compressional type. The resonance behaviour of shear waves is similar, however[2].

b) Computer Simulation of Actual Lattice

Of course, the HERA electron and proton magnet lattices are in reality no pure periodic FODO structures. The difference is mainly due to the straight sections with low beta section, spin rotators, rf sections, and so on, installed. Using the PETROS optics program[5] as a subroutine, computer simulation of the actual HERA lattices to single ground waves has been performed. Three types of straight ground waves has been investigated: vertical, horizontal compressional, horizontal shear. A ground wave amplitude of 0.1 mm has been applied in all cases, and the closed orbit response amplitude has been extracted from the PETROS output. The results are shown in figs. 30-36. Since a single wave is simulated, the results depend on the wave's direction and phase. It is illustrated by fig. 31 (in comparison with fig. 30) that this is a minor effect, however. If figs. 30-36 are compared with the corresponding results of analytical investigations (figs. 28, 29), it is seen that the overall agreement is quite good. The conclusion is that the HERA lattices are fairly well modelled by periodic FODO lattices as far as ground waves are concerned.

6. CONCLUSIONS

Precise prediction of the closed-orbit motion requires – in principle – total knowledge of the motion of each of the quadrupole magnets (not to speak of all the other mechanisms which move the orbit). This information is, of course, not attainable for HERA. With measurements and model calculations as reported in this paper, however, one can estimate the beam separation due to fast ground motion within an error factor of, say, 2. From model calculations it is seen that ground waves with $C/\lambda < 20$ (i.e. $\lambda > 300$ m) will affect neither the electron nor the proton closed orbit, corresponding to frequencies ≤ 3 Hz. For larger frequencies, typical rms ground motion amplitudes of 0.2 μm have been found. Elastic behaviour of the quadrupole magnet supports amplifies this by a factor of 2 or 4-5 in the vertical or horizontal directions, respectively, i.e. rms quadrupole motion amplitudes are:

electron ring:	1.0 μm (hor)	0.4 μm (vert)
proton ring (preliminary):	0.8 μm (hor)	0.4 μm (vert)

The closed orbit response can be estimated from paragraph 5, if HERA beta-function values at the interaction points are allowed for:

β^* (electrons): $\beta_x = 2$ m $\quad \beta_z = 0.7$ m

β^* (protons): $\beta_x = 10$ m $\quad \beta_z = 1.0$ m

For wavelengths $\lambda > 60$ m ($C/\lambda < 100$, $\nu \leq 20$ Hz) it is seen that the response (almost) never exceeds the value for uncorrelated motion by more than 50 %. Since $\nu > 20$ Hz contributions are small in all spectra, we take the 1.5 × uncorrelated motion value as an upper limit. It will not be too pessimistic, since probably the correlation of the ground motion will be destroyed by the individual response of each support anyway. The expected closed-orbit response at the interaction points will be therefore

electron c.o. response at IP:	14 (hor)	8 (vert)
proton c.o. response at IP:	18 (hor)	6 (vert)

From this, the rms *separation* amplitude will be:

$$\sqrt{(14 \cdot 1\ \mu m)^2 + (18 \cdot 0.8\ \mu m)^2} = 20\ \mu m \qquad \text{(horizontal)}$$

$$\sqrt{(8 \cdot 0.4\ \mu m)^2 + (6 \cdot 0.4\ \mu m)^2} = 4\ \mu m \qquad \text{(vertical)}$$

Vertical separation will be increased by about 50 % during working hours, and on top of all that there will be events of approx. 5 sec duration which will increase these values by a factor of two. During working hours these events will occur at a rate of approx. 1-2 per minute.

These results must be compared with beam sizes at the interaction point:

electrons, 26 GeV, $\varepsilon_z/\varepsilon_x = 0.05$: $\sigma_x = 270\ \mu m$, $\sigma_z \approx 37\ \mu m$

protons, 820 GeV: $\sigma_x = 260\ \mu m$, $\sigma_z \approx 70\ \mu m$

It is seen that the effect of beam separation on luminosity will be certainly few percent only.

The uncertainty is about a factor of two. This is due to assumptions concerning ground motion velocity, correlation of magnet motion, and superconducting magnet motion under realistic operation conditions. A number of measurements are under way to clarify these questions.

7. ACKNOWLEDGEMENT

The author is indebted to Prof. Dr. J. Klußmann (Universität Hamburg) for valuable advice and lending seismometer equipment. He wishes to thank Dr. R. Brinkmann, L. Graetke, and Dr. T. Limberg for discussions and assistance.

References

[1] **T. Aniel, J.L. Laclare**: Sensitivity of the ESRP machine to ground movement, LNS/086 (1985)

[2] **J. Roßbach**: Closed Orbit Distortions of Periodic FODO Lattices due to Plane Ground Waves, DESY M-87-09 and Part. Acc. Vol. 23, No 2 (1988)

[3] **Martin Steinwachs**: Systematische Untersuchungen der kurzperiodischen seismischen Bodenunruhe in der Bundesrepublik Deutschland, Geologisches Jahrbuch, Reihe E (Geophysik), 3, 1974

[4] **G.E. Fischer** and **P. Morton**: Ground Motion tolerances for the SSC, SLAC-PUB-3870, 1986

[5] **J. Kewisch**: Diplomarbeit, Hamburg 1976

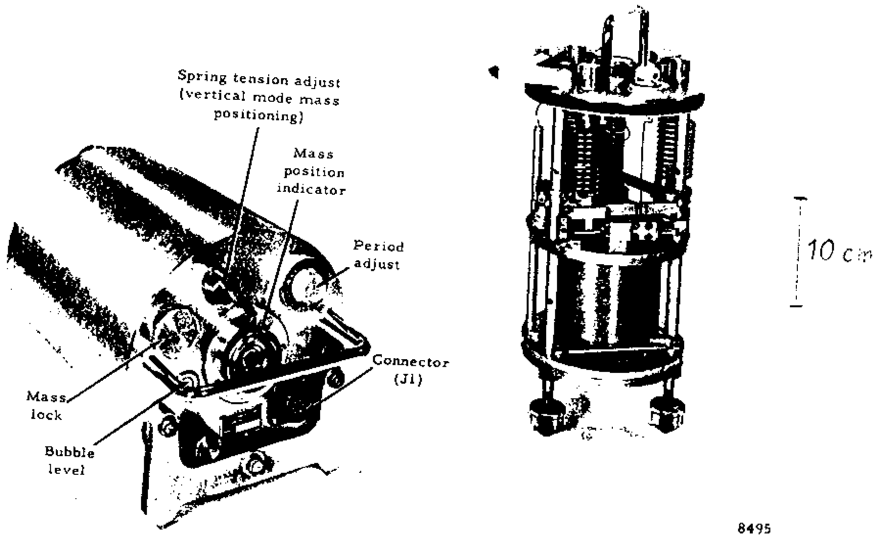

Figure 1. Portable Short-Period Seismometer, Model 18300

Fig. 1 Portable Short-Period Seismometer, Model 18300 by Teledyne Geotech, USA.

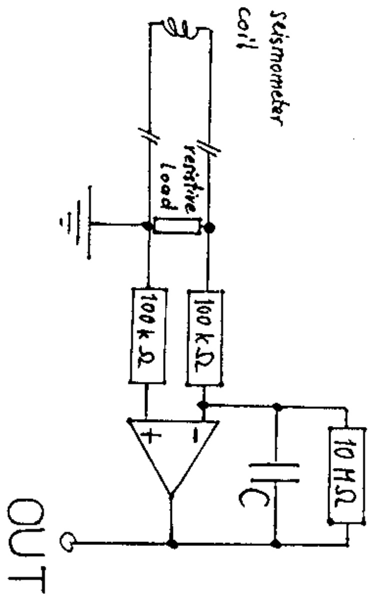

Fig. 2 Circuitry for damping and integration. Capacitors C = 0.01 μF and 0.15 μF have been used, i.e. integrator time constants are $\tau = 1\ ms$ or $\tau = 15\ ms$, respectively.

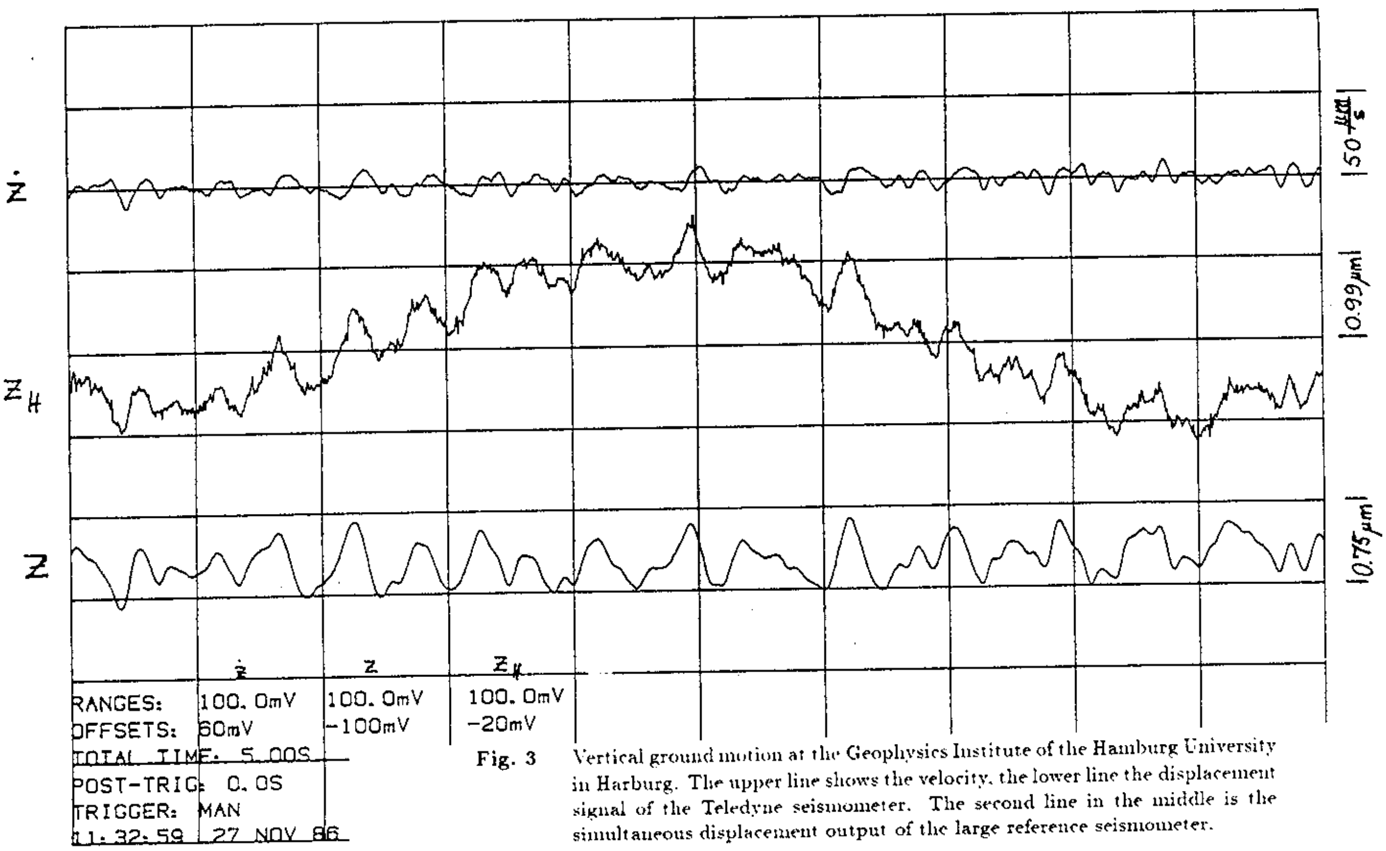

Fig. 3 Vertical ground motion at the Geophysics Institute of the Hamburg University in Harburg. The upper line shows the velocity, the lower line the displacement signal of the Teledyne seismometer. The second line in the middle is the simultaneous displacement output of the large reference seismometer.

$\tau = 15\ ms$

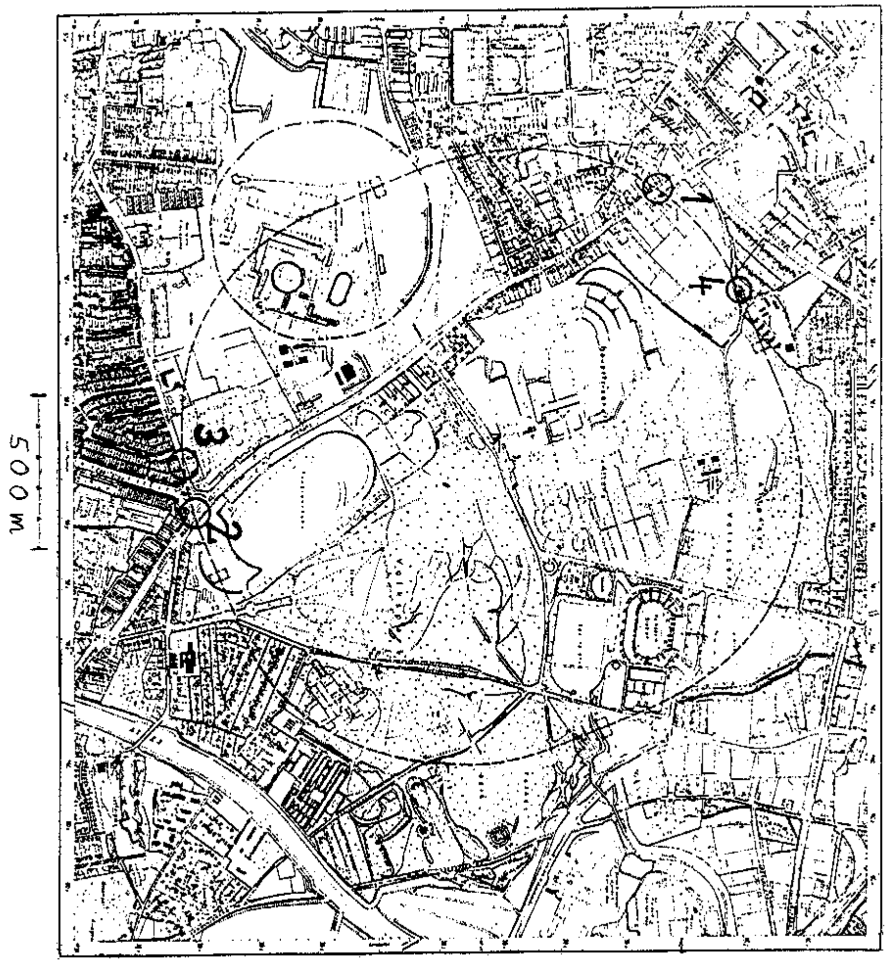

Fig. 4 Location of the HERA storage ring. Positions where ground motion data have been taken in the HERA tunnel are indicated 1, 2, 3, 4.

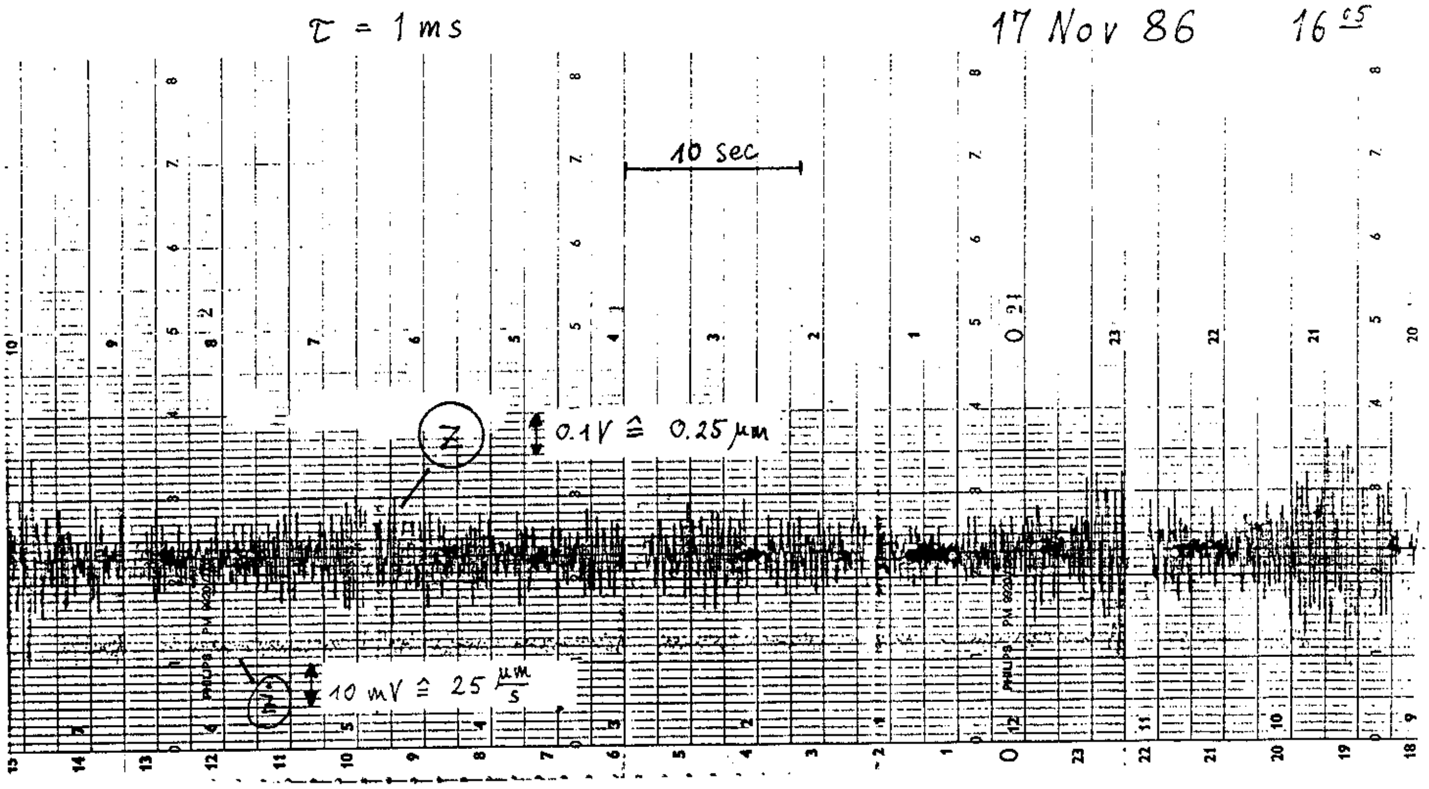

Fig. 5 Vertical motion of the HERA tunnel floor (at point 2 of fig. 4). Large amplitudes are suppressed by approx. 10 % due to mechanical inertia of the recorder.

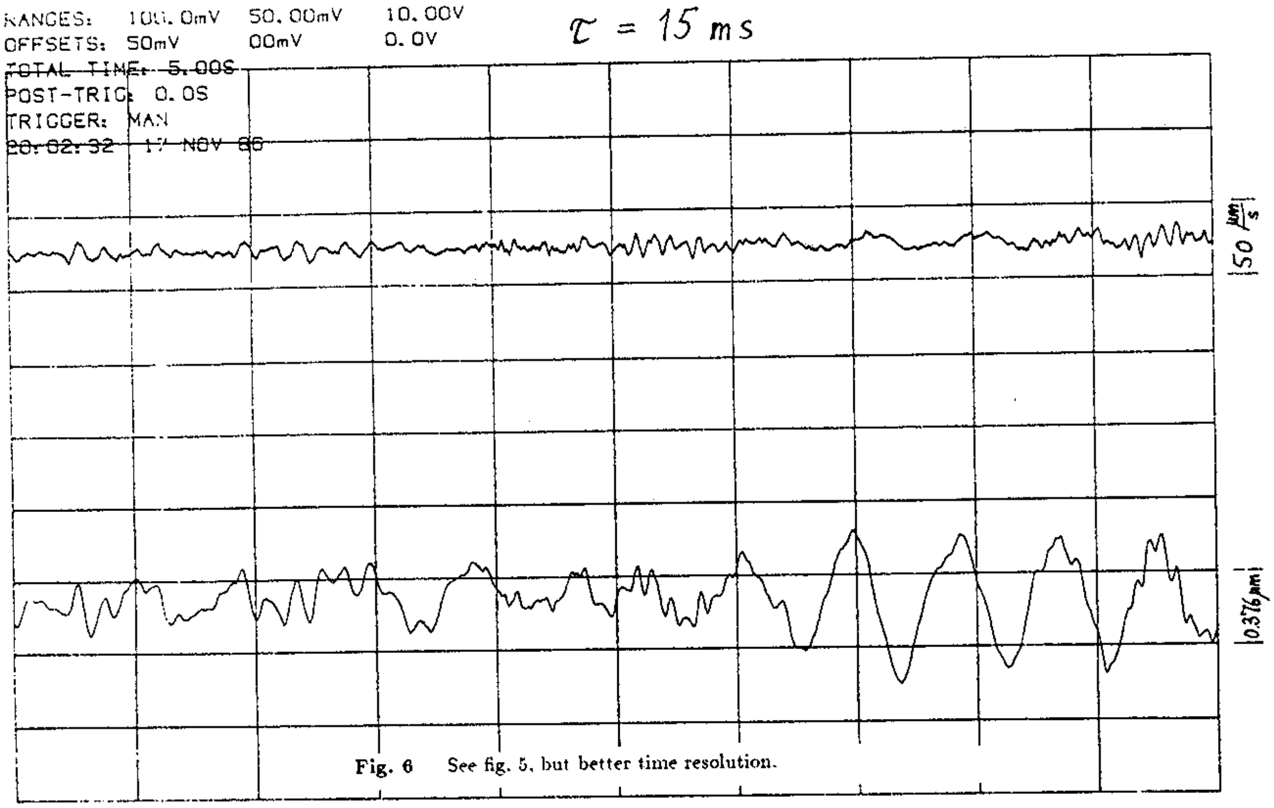

Fig. 6 See fig. 5, but better time resolution.

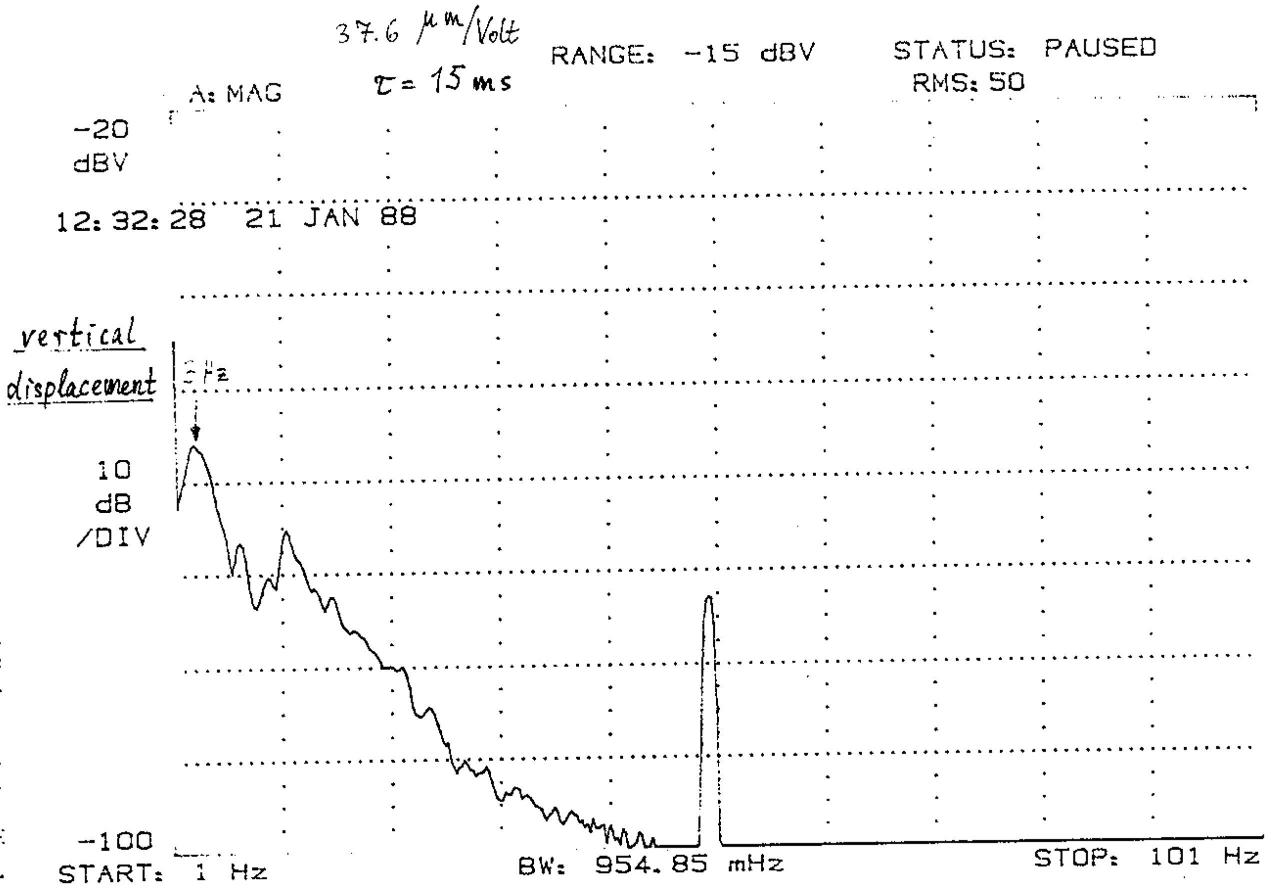

Fig. 7 Ten minutes average spectrum of vertical tunnel displacement at position 1.

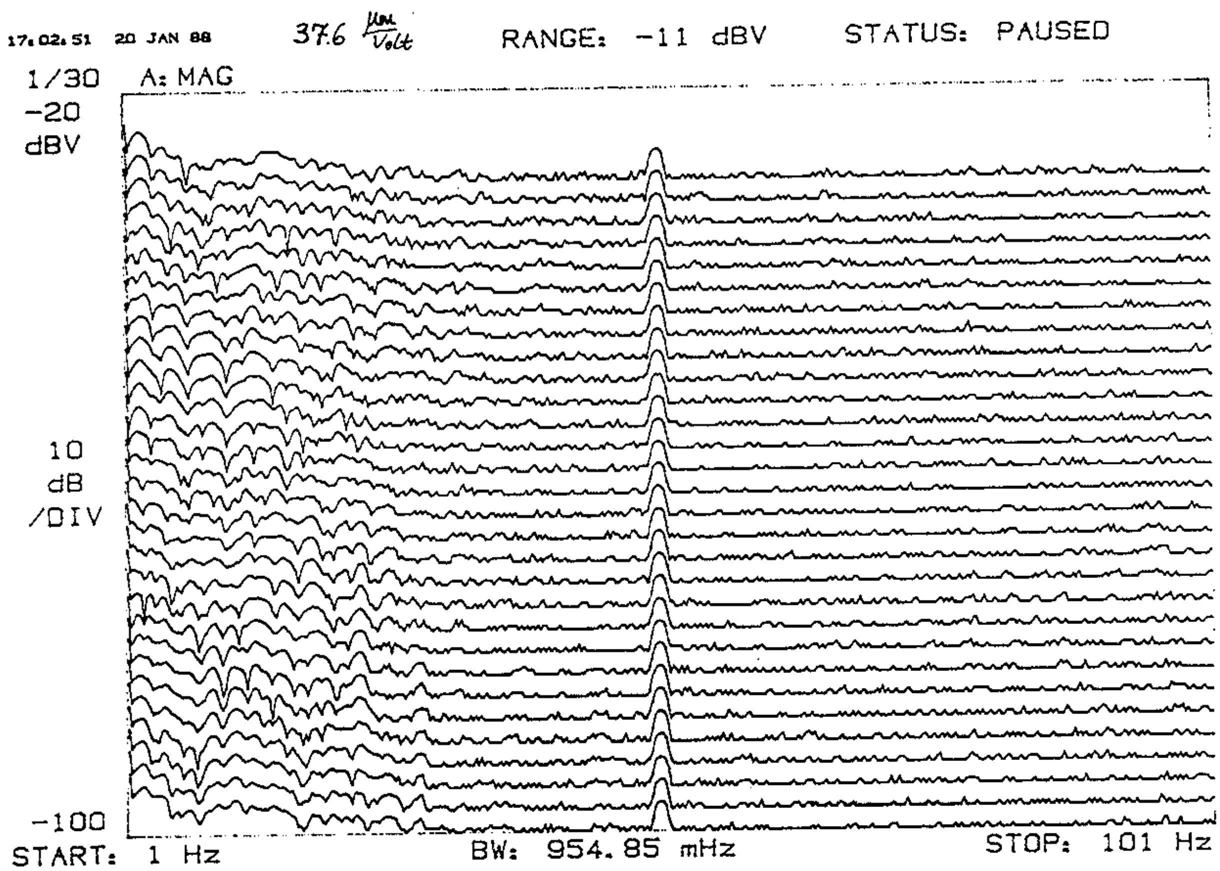

Fig. 8 Map representation of 30 FFTs of vertical tunnel displacement at position 1.

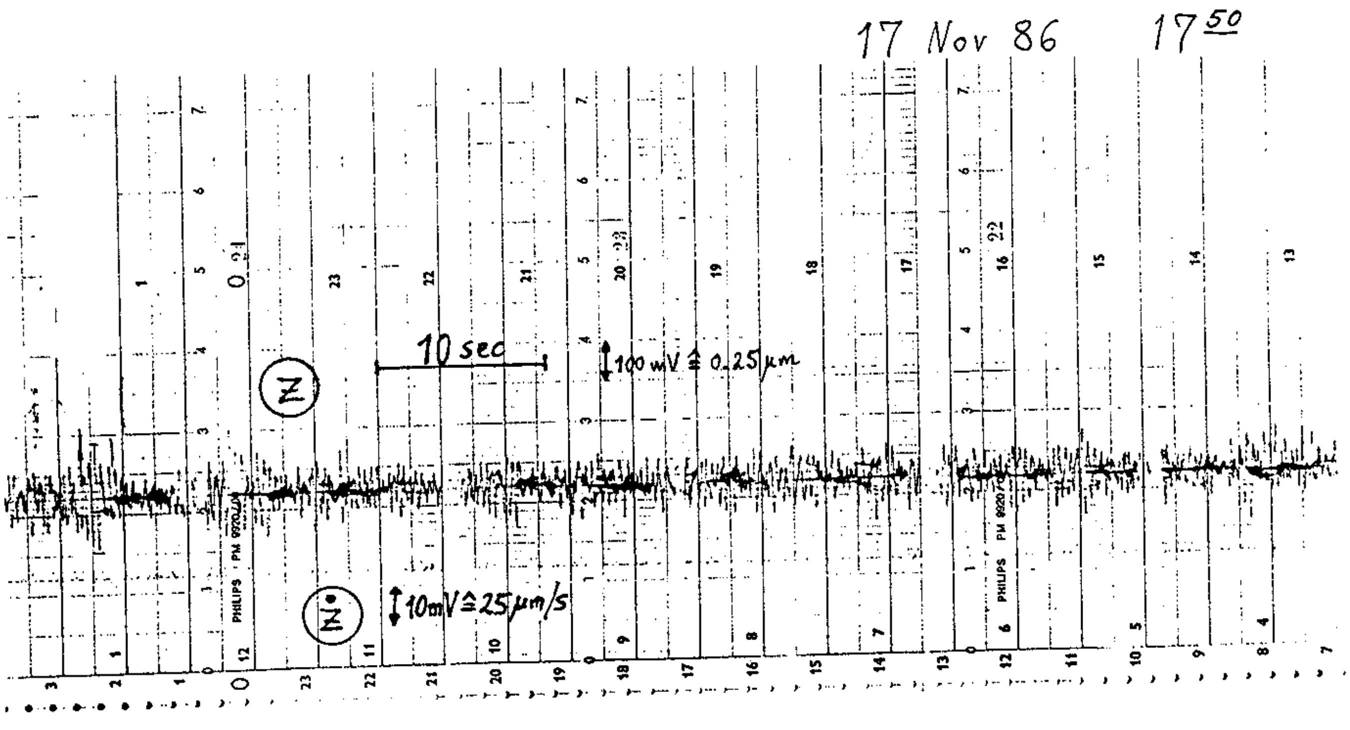

Fig. 9 Vertical motion of the HERA tunnel floor at point 3 (see fig. 4).

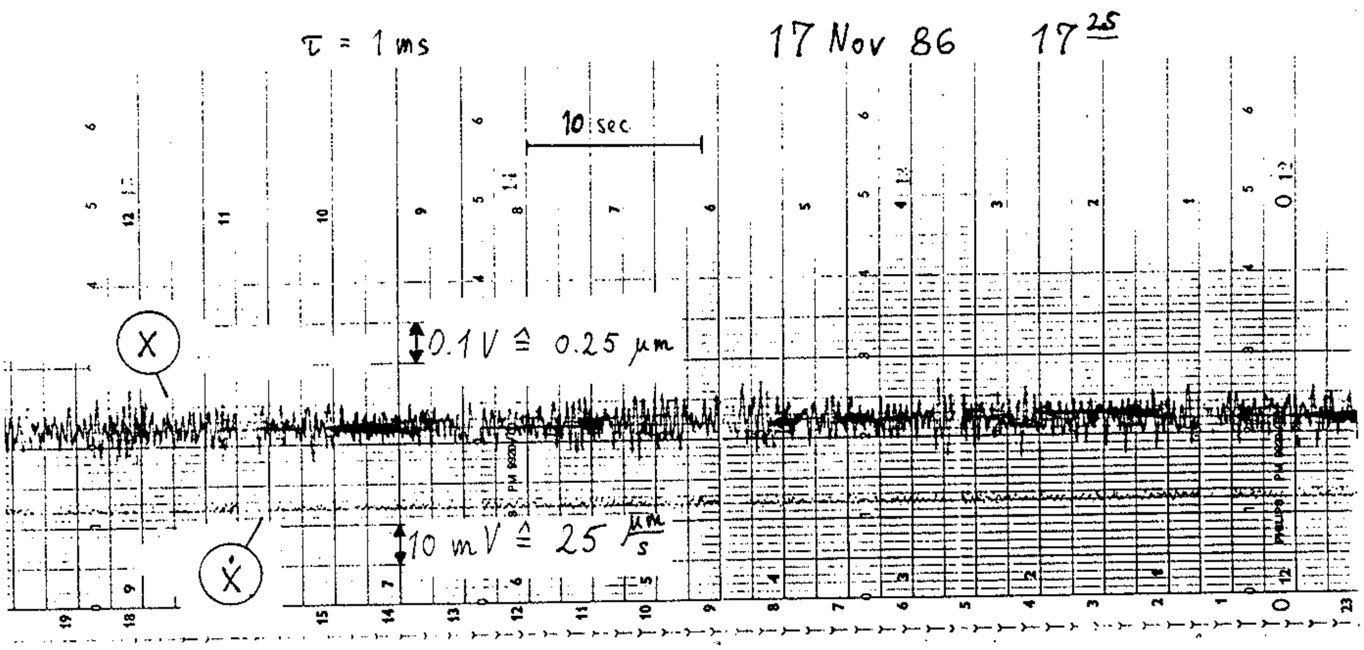

Fig. 10 Horizontal motion (perpendicular to beam axis) of the HERA tunnel floor at point 3 (see fig. 4).

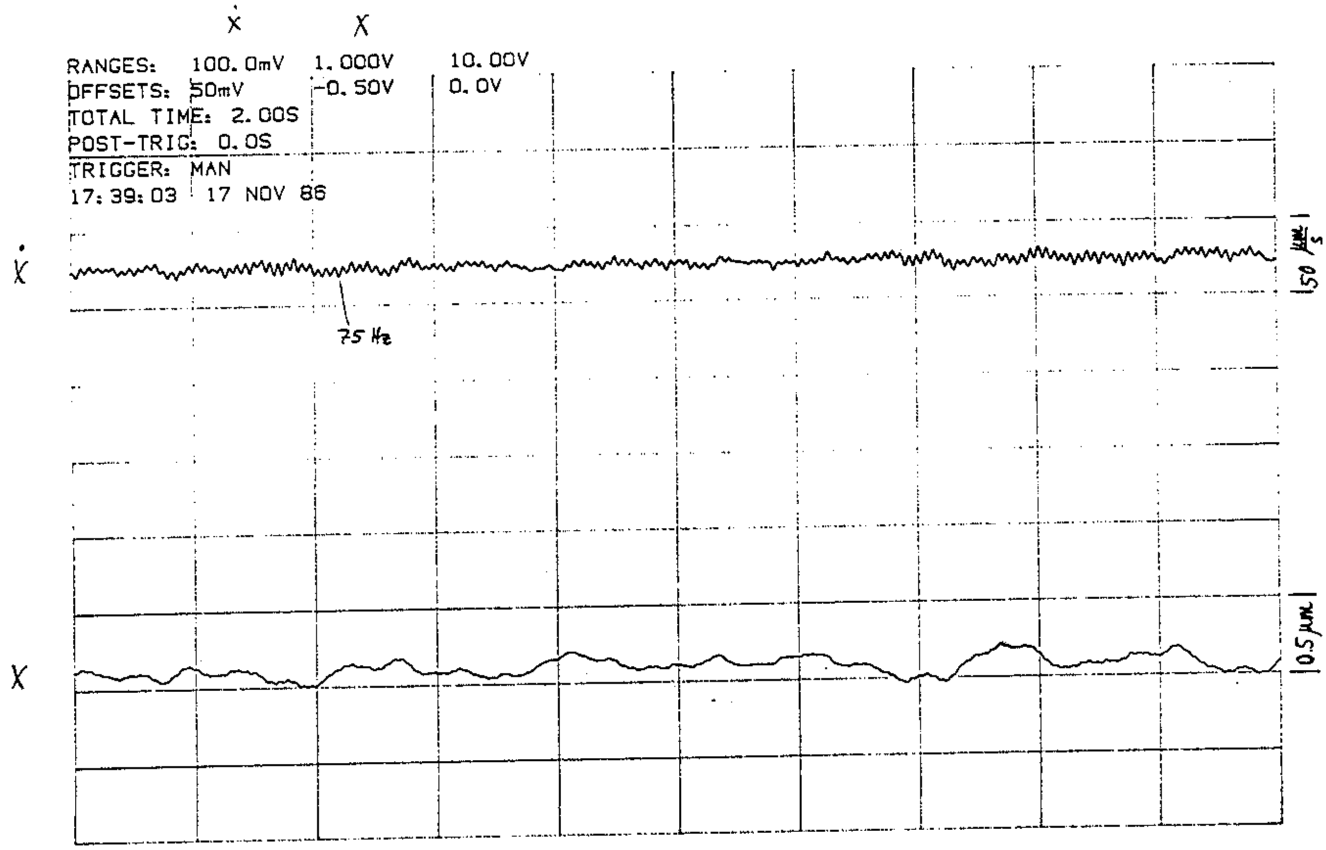

Fig. 11 See fig. 10, but better time resolution.

typical horizontal motion at pos. 3

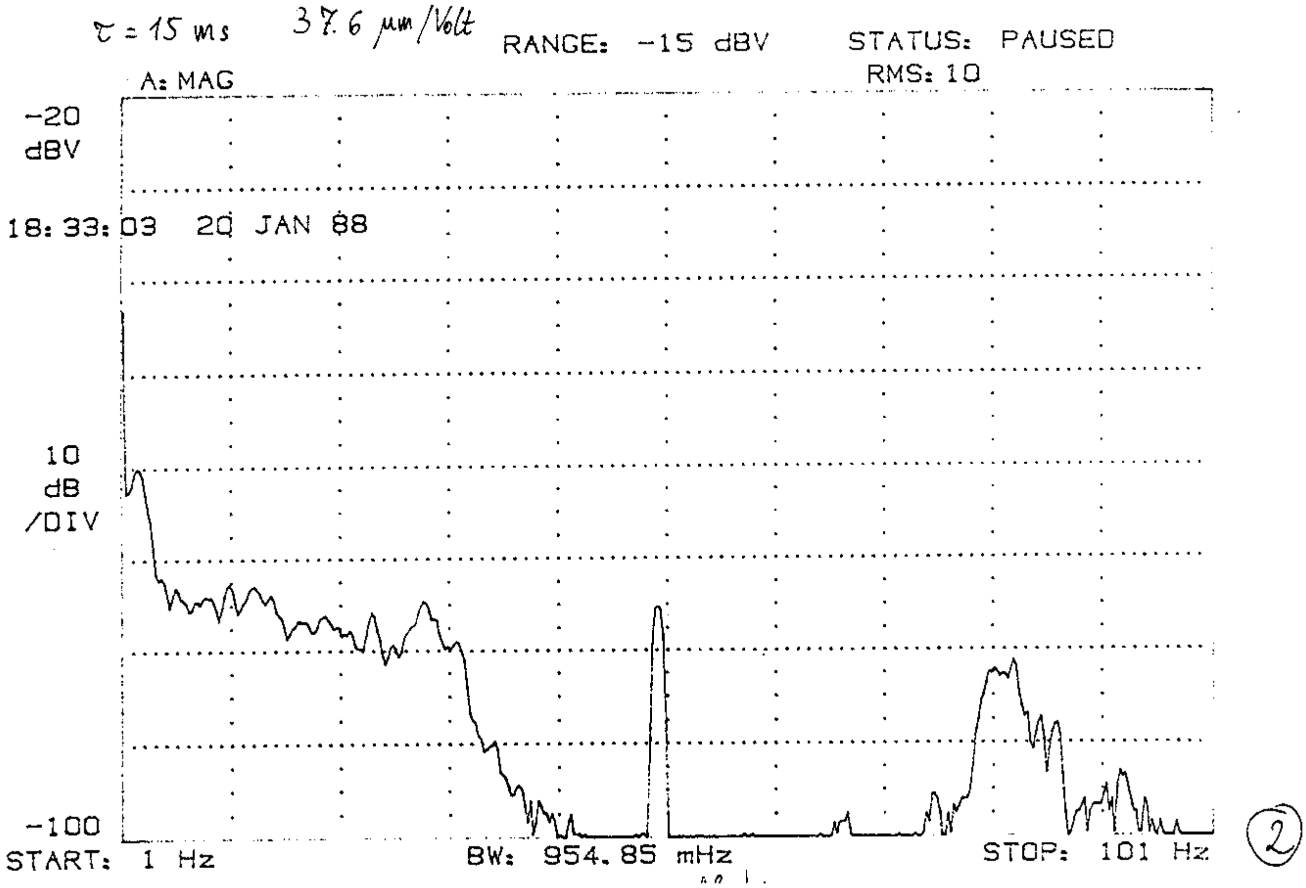

Fig. 12 Two minutes averaged spectrum of horizontal tunnel displacement at position 1.

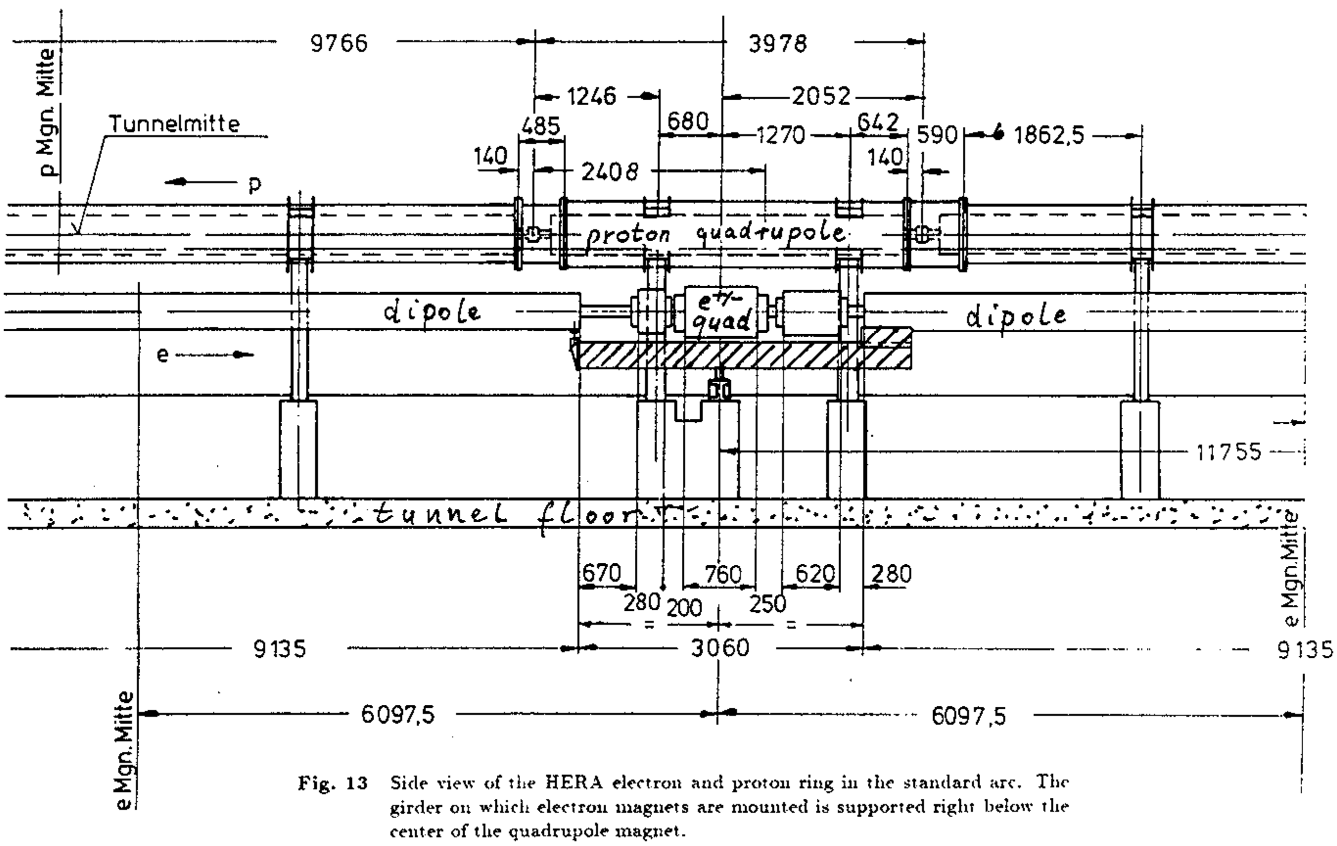

Fig. 13 Side view of the HERA electron and proton ring in the standard arc. The girder on which electron magnets are mounted is supported right below the center of the quadrupole magnet.

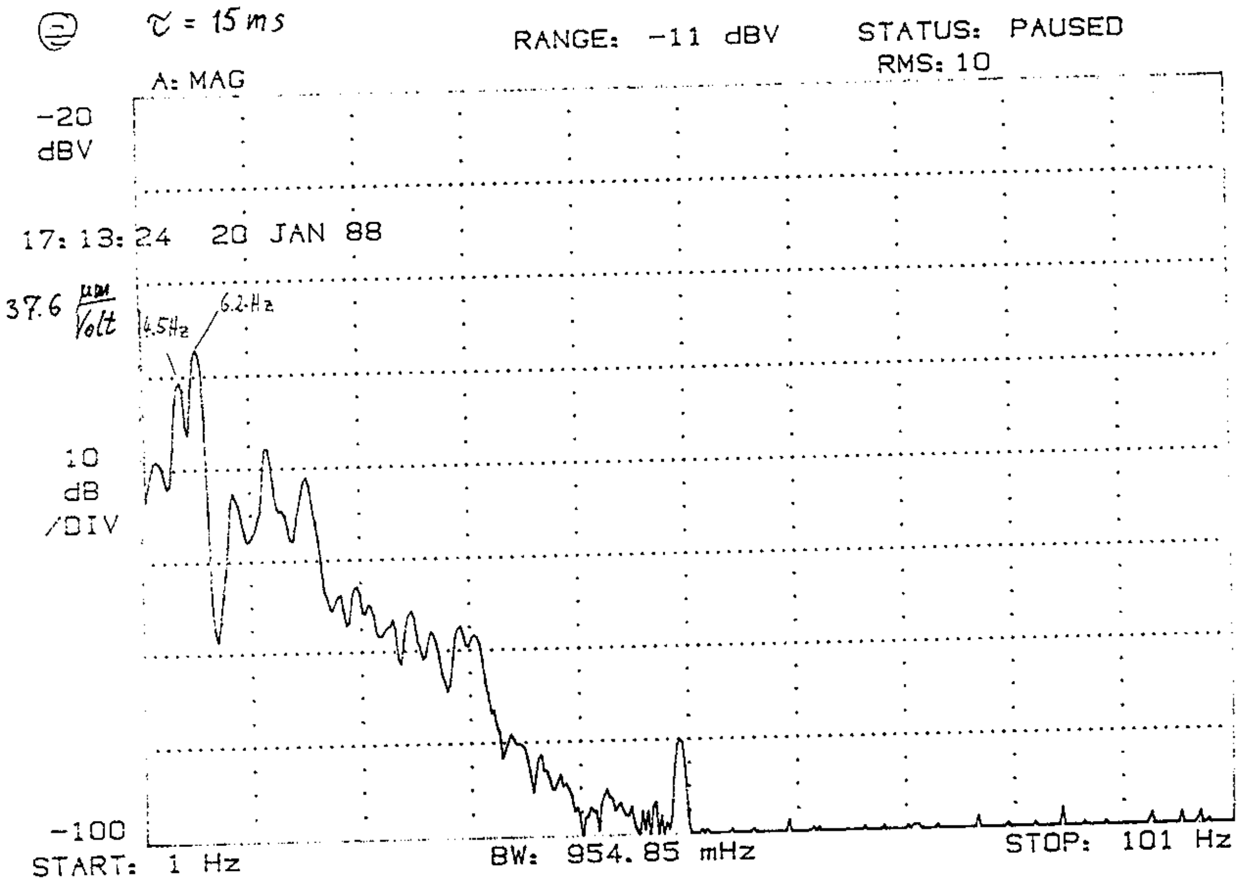

Fig. 14 Vertical displacement spectrum of the girder on which the electron ring magnets are mounted. The seismometer was placed about 1 m downstream from the quadrupole center (627 m left from IP North, see point 1 in fig. 4).

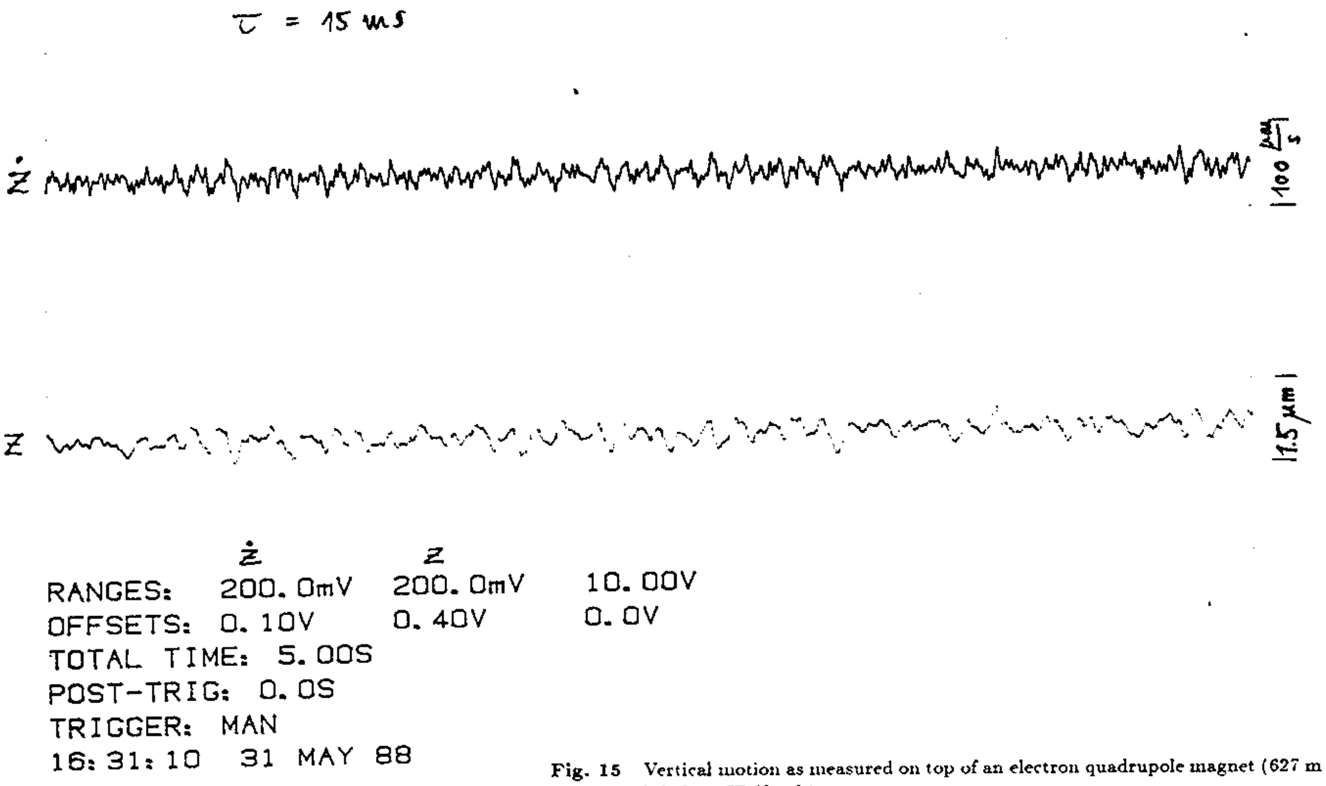

Fig. 15 Vertical motion as measured on top of an electron quadrupole magnet (627 m left from IP North).

Fig. 16 See fig. 15 (motion on top of e-quad), ten minutes average spectrum. To be compared with fig. 7 (ground motion).

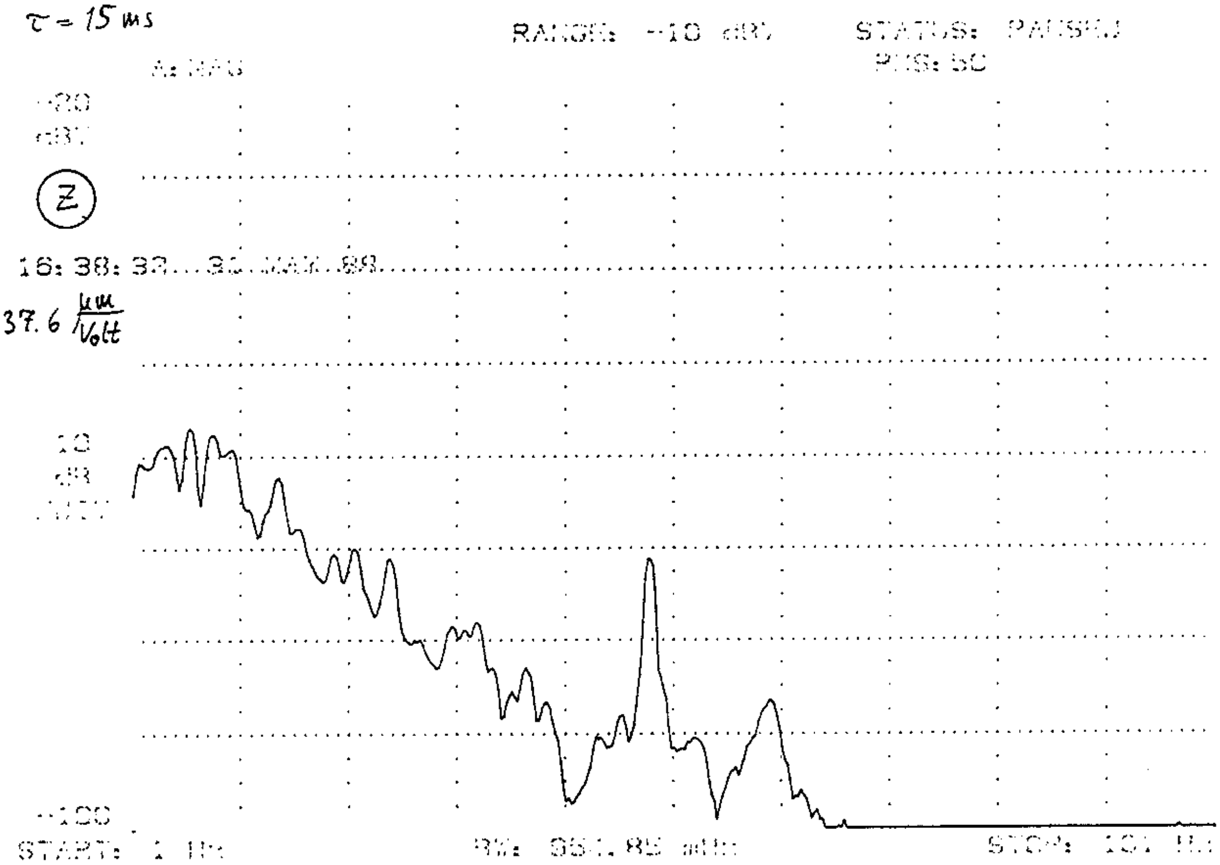

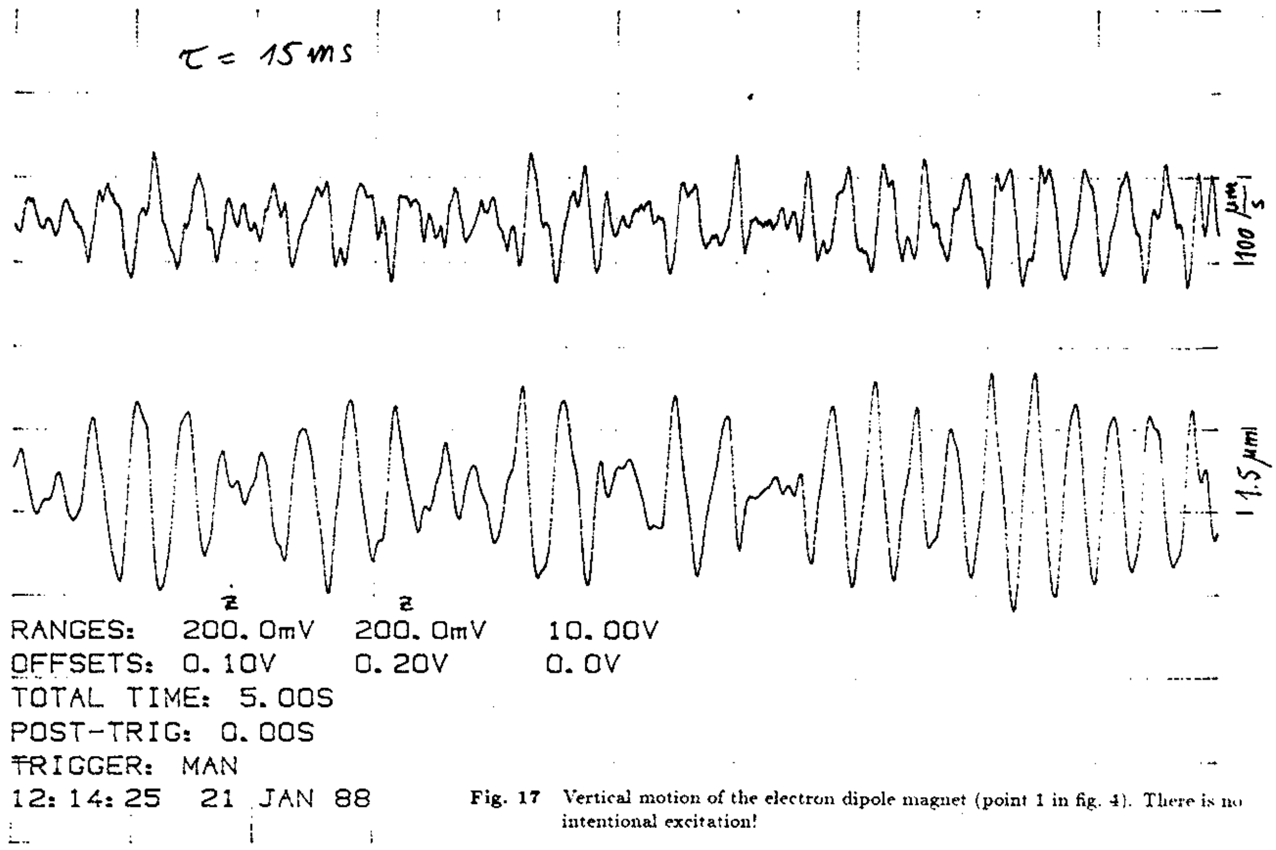

Fig. 17 Vertical motion of the electron dipole magnet (point 1 in fig. 4). There is no intentional excitation!

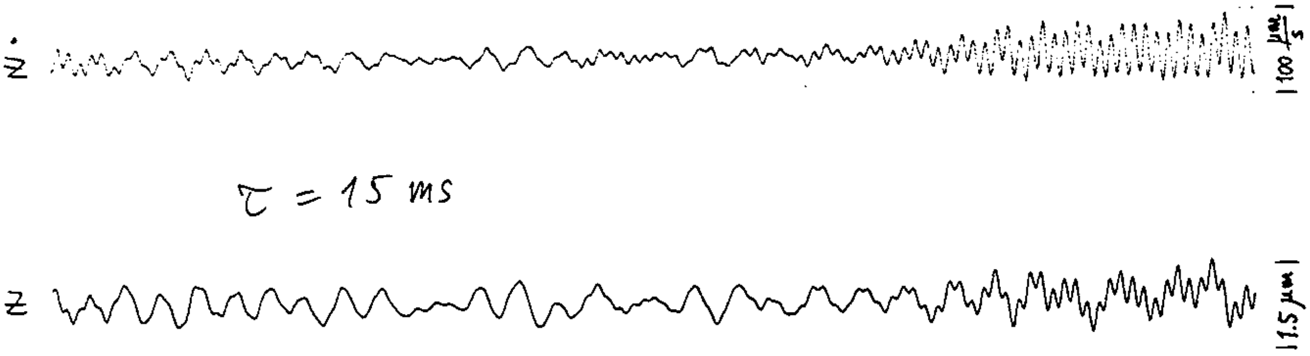

	ż	z	
RANGES:	200.0mV	200.0mV	10.00V
OFFSETS:	0.10V	0.40V	0.0V

TOTAL TIME: 5.00S
POST-TRIG: 0.0S
TRIGGER: MAN
08:20:05 01 JUN 88

Fig. 18 Vertical motion of the electron quadrupole 197 m left from IP North (point 4 in fig. 4) on a special type of support (see text).

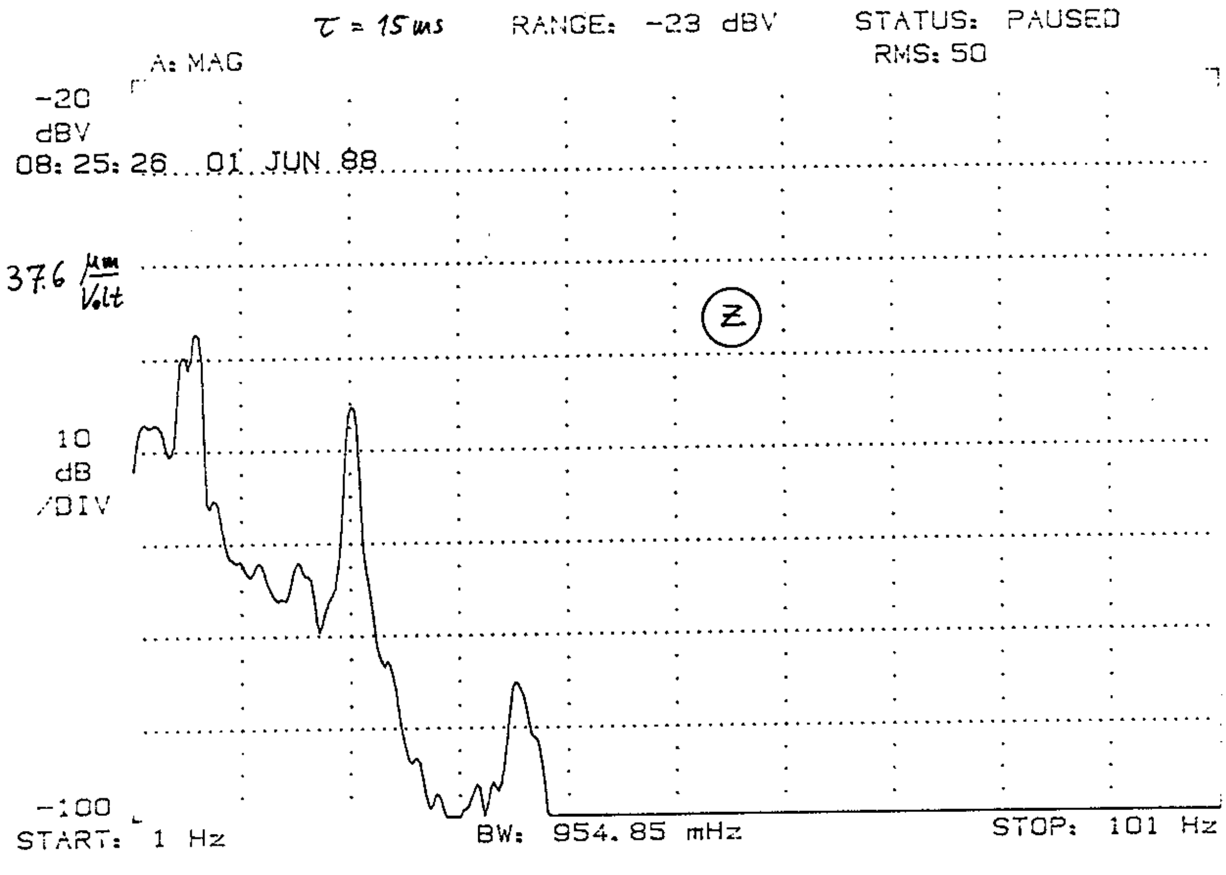

Fig. 19 See fig. 18, ten minutes average spectrum of vertical displacement.

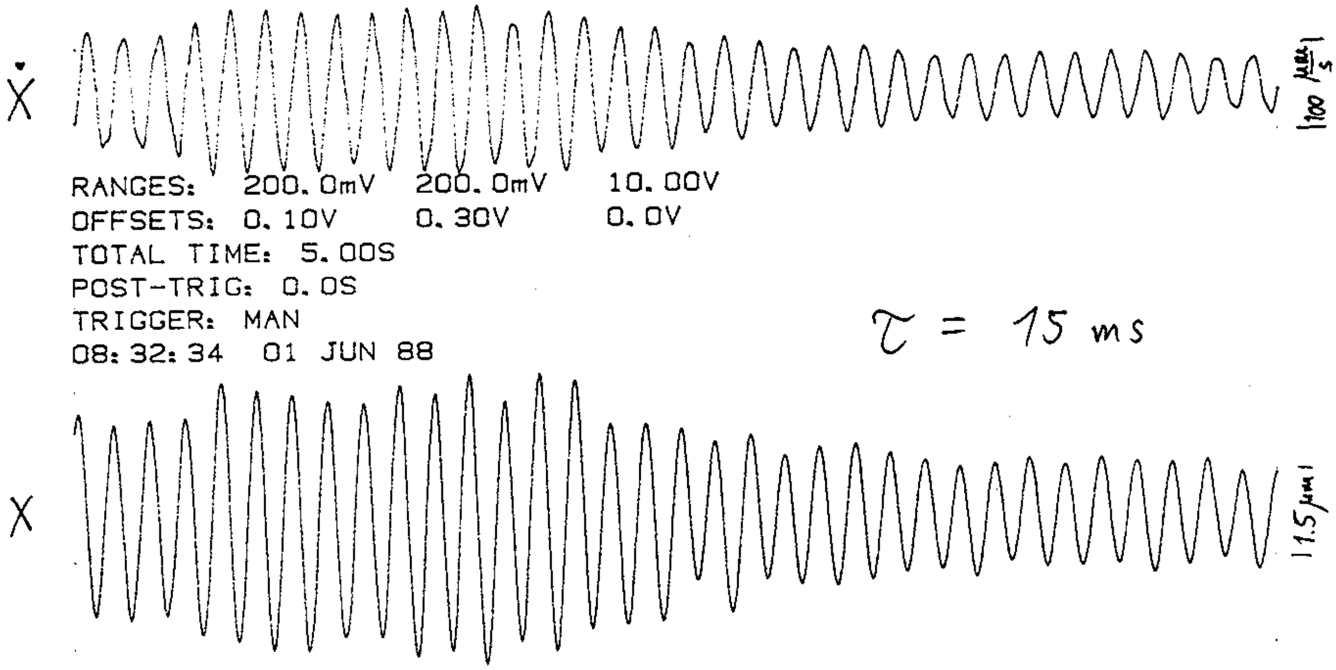

Fig. 20 See fig. 18, but horizontal motion.

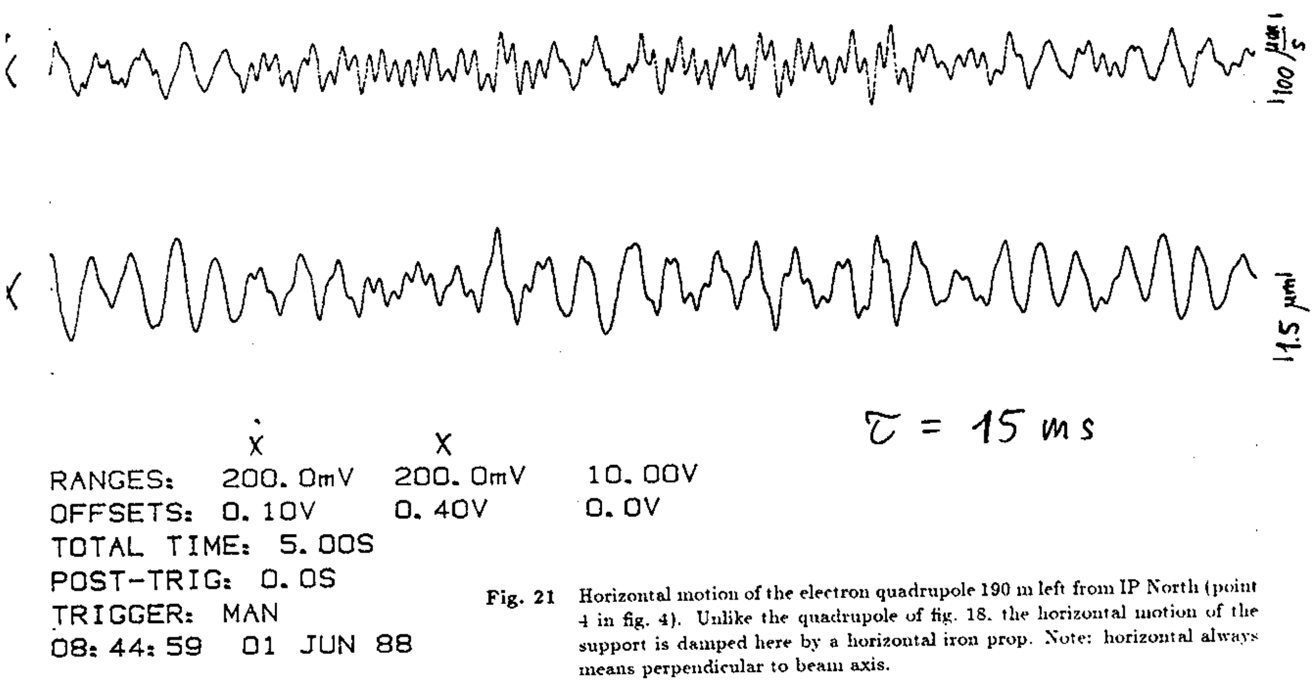

Fig. 21 Horizontal motion of the electron quadrupole 190 m left from IP North (point 4 in fig. 4). Unlike the quadrupole of fig. 18, the horizontal motion of the support is damped here by a horizontal iron prop. Note: horizontal always means perpendicular to beam axis.

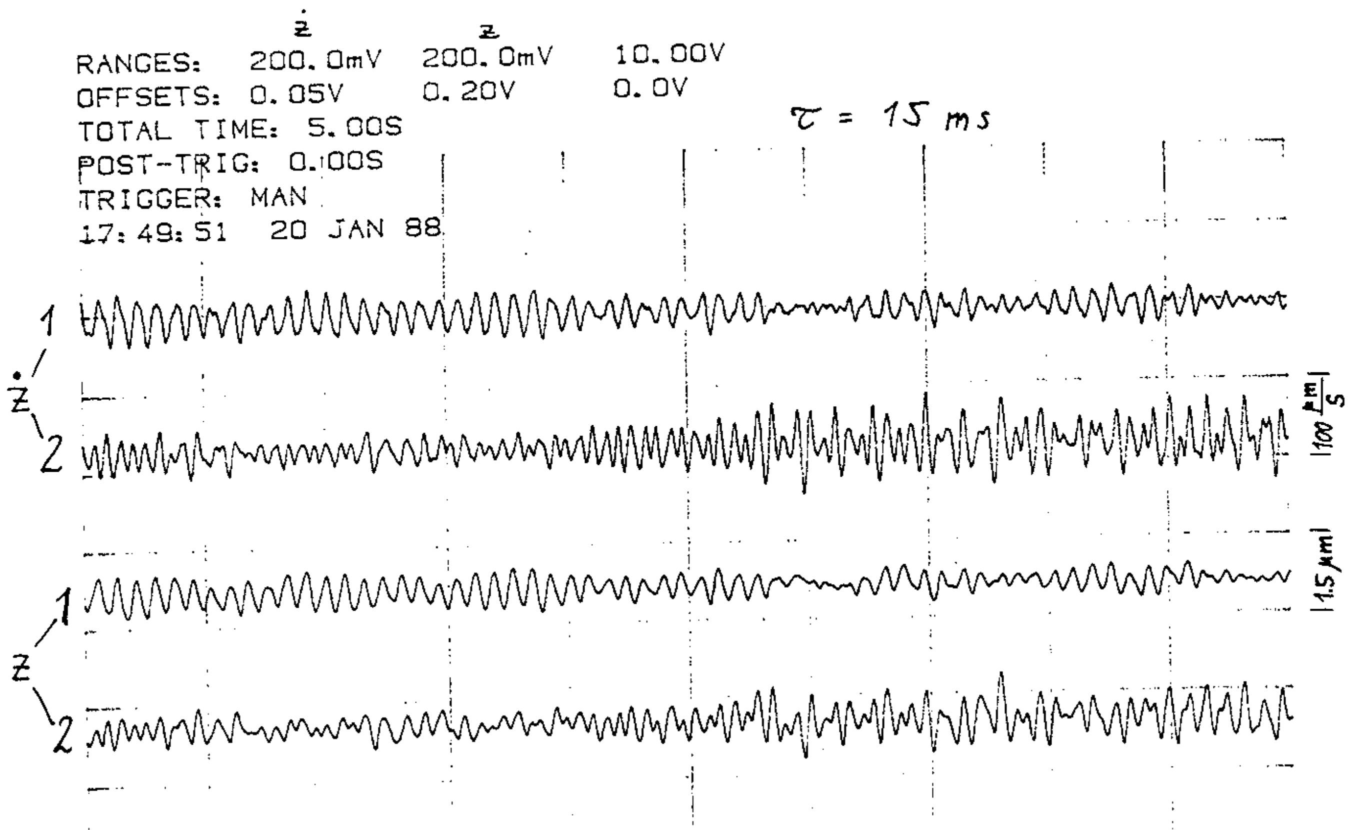

Fig. 22 Two 5 sec periods of vertical motion on top of a proton quadrupole cryostat, no Helium flowing, magnet at room temperatur (see text).

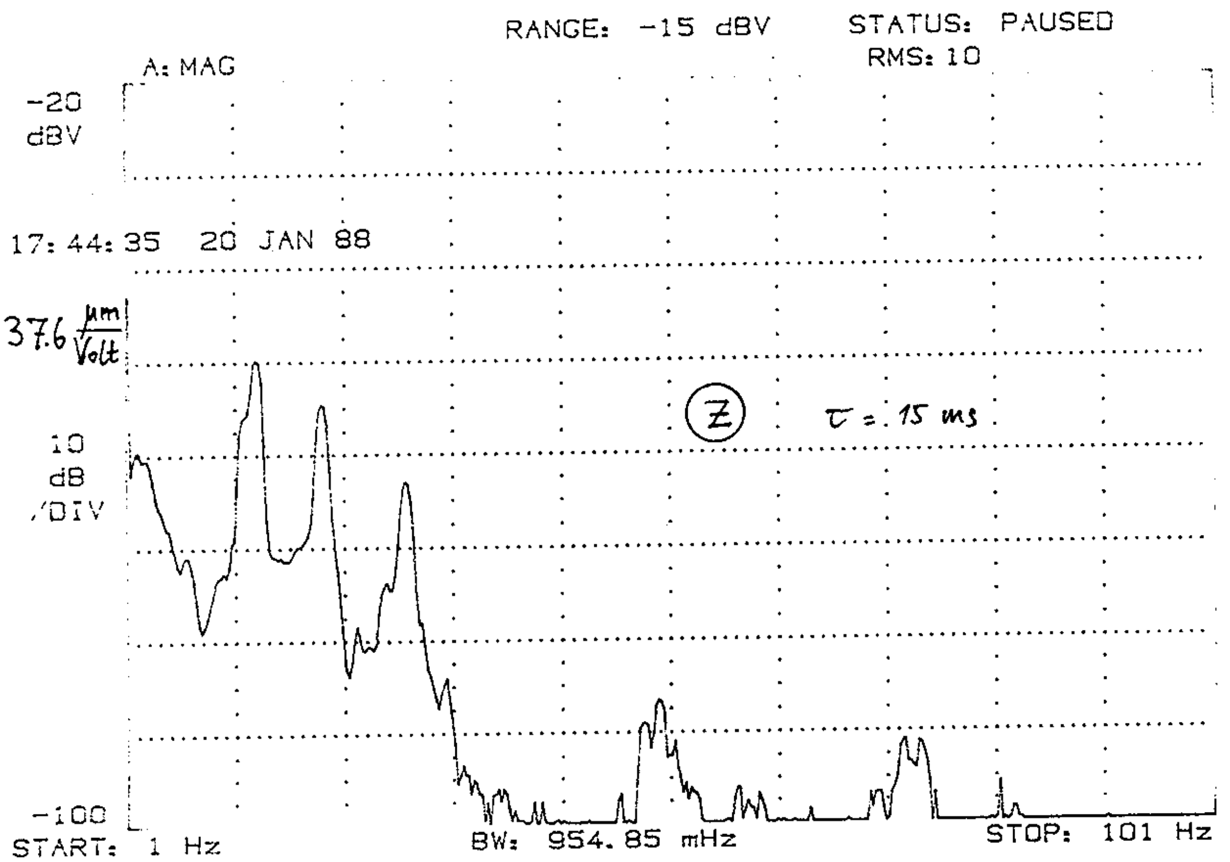

Fig. 23 Spectrum of vertical displacement, see fig. 22.

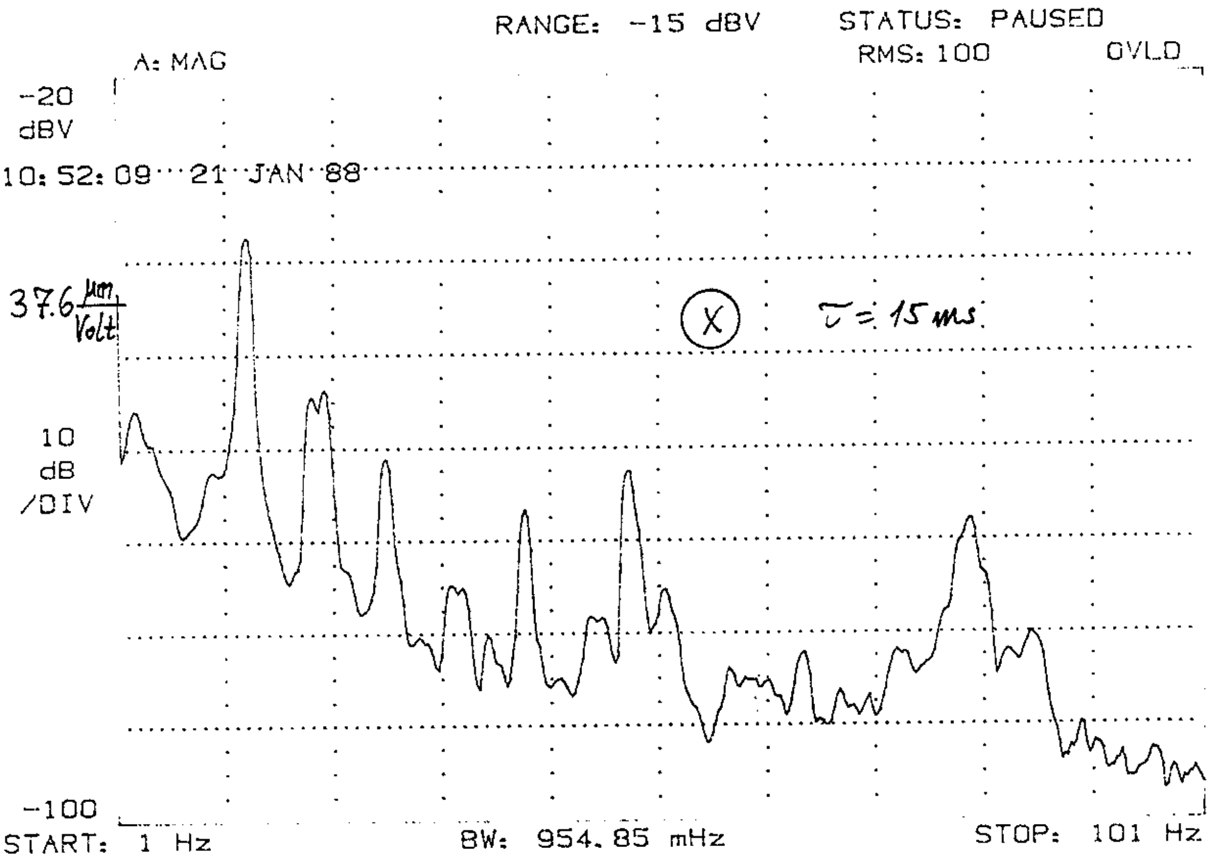

Fig. 24 Spectrum of horizontal displacement. see fig. 22.

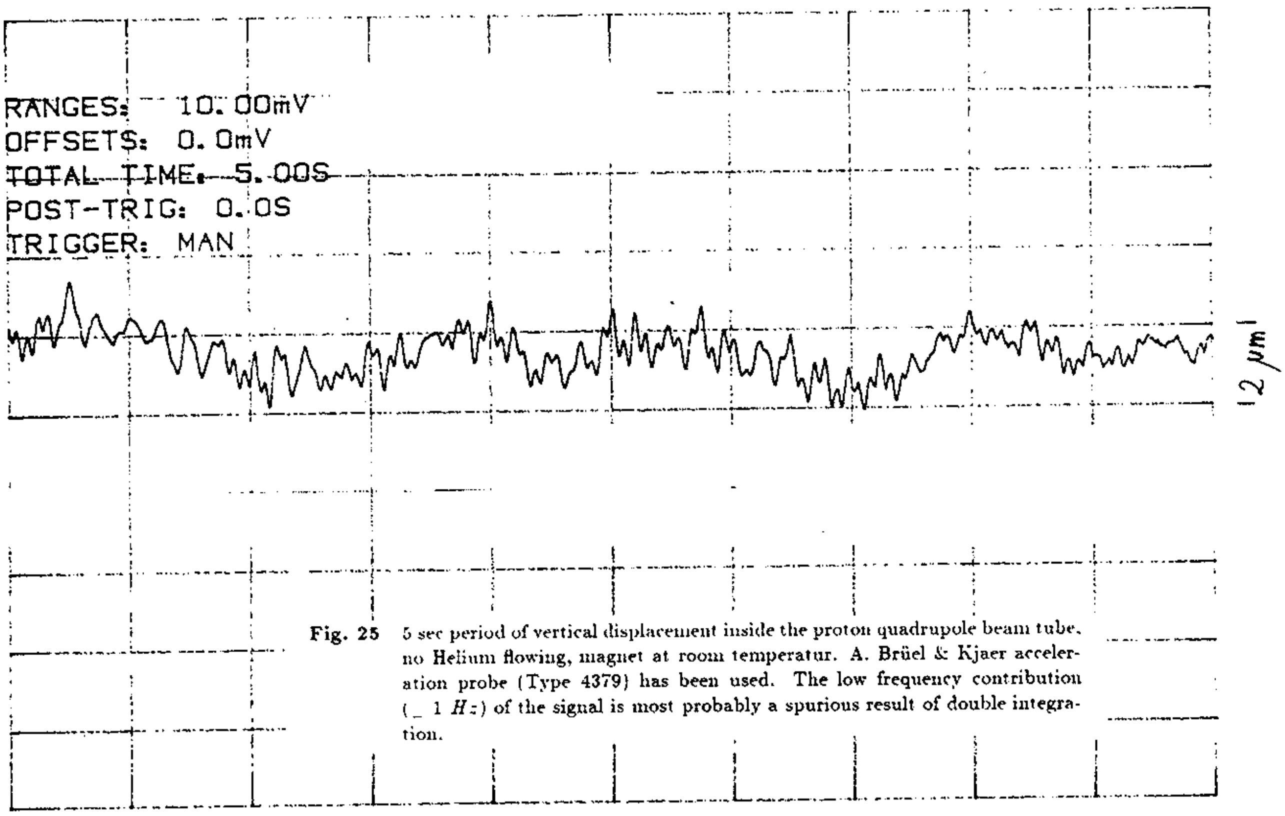

Fig. 25 5 sec period of vertical displacement inside the proton quadrupole beam tube, no Helium flowing, magnet at room temperatur. A. Brüel & Kjaer acceleration probe (Type 4379) has been used. The low frequency contribution ($\_$ 1 Hz) of the signal is most probably a spurious result of double integration.

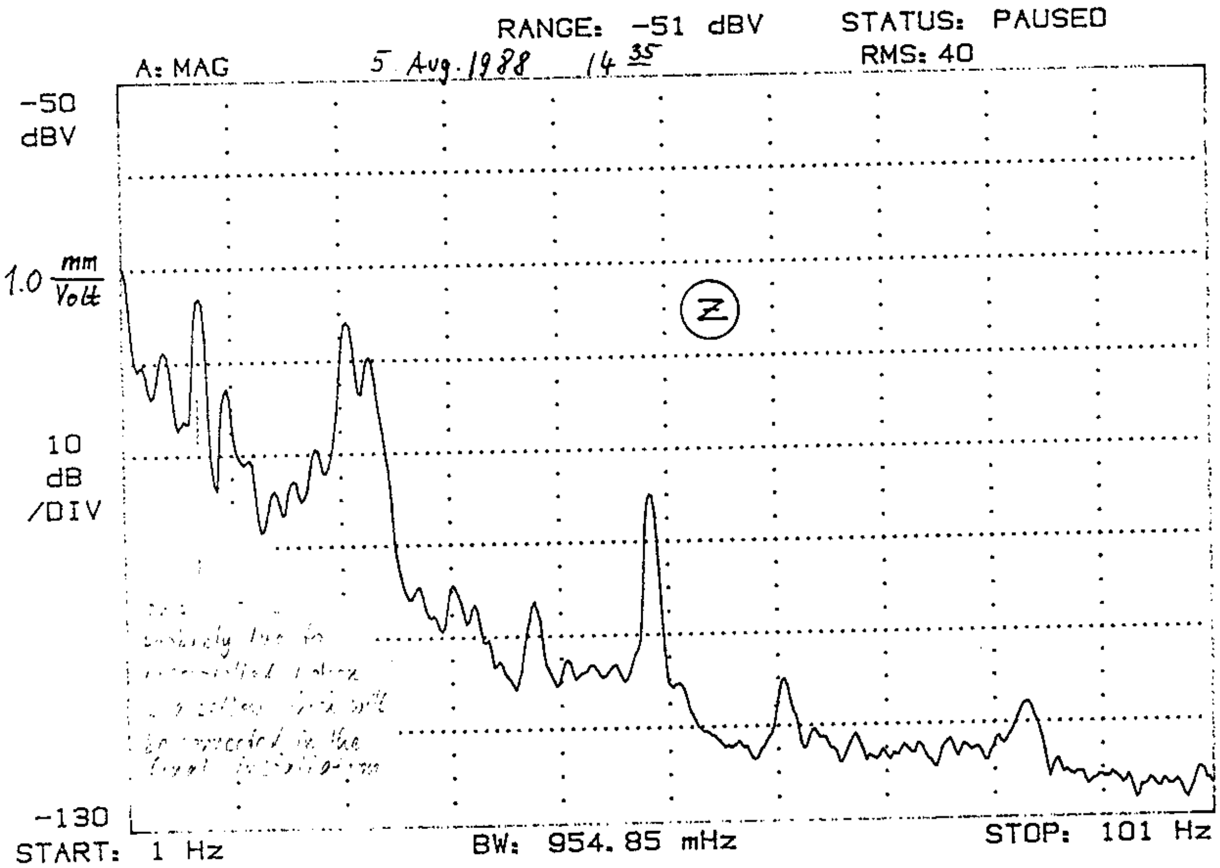

Fig. 26 Vertical displacement spectrum inside the proton quadrupole beam tube, see fig. 25.

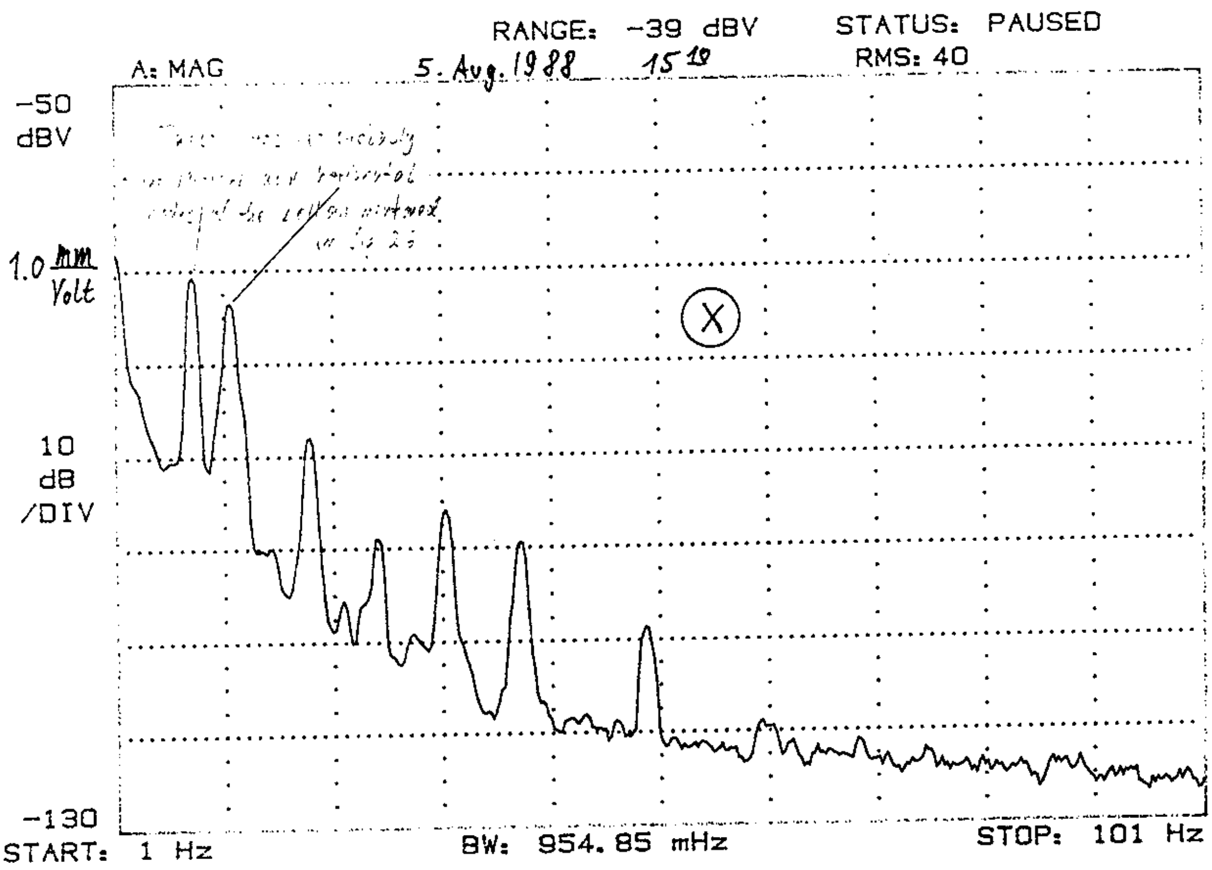

Fig. 27 Horizontal displacement spectrum inside the proton quadrupole beam tube, see fig. 25.

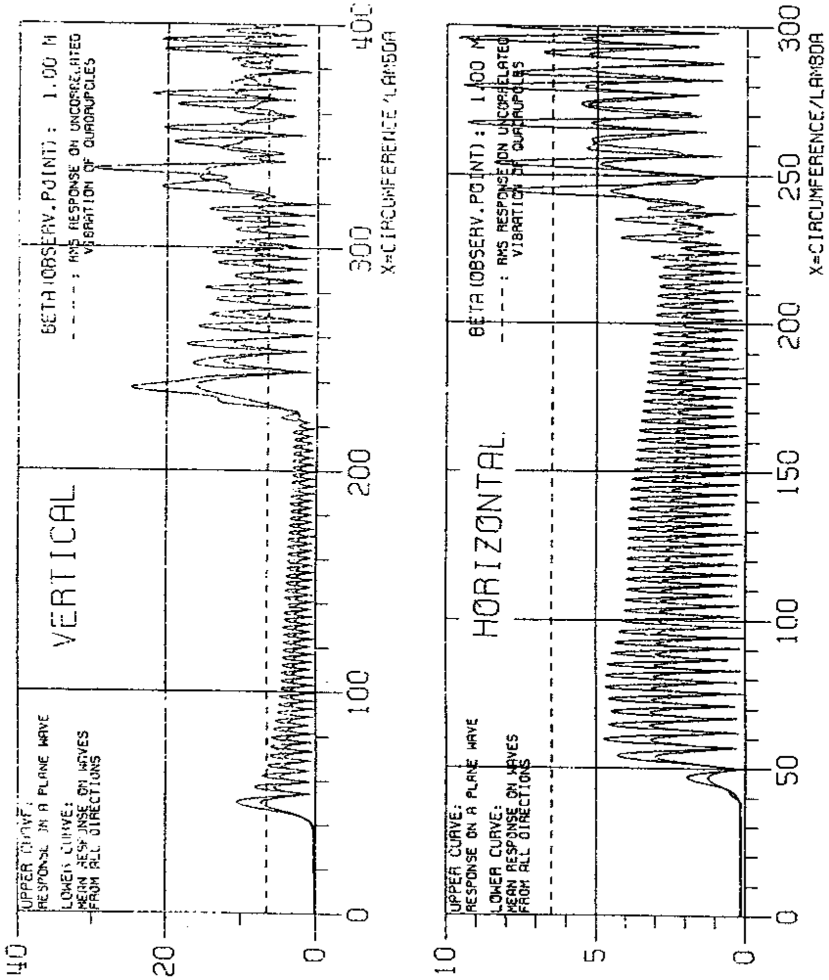

Fig. 28 Closed orbit response of a model periodic FODO lattice to plane ground waves of wave length λ. For the HERA electron ring, $N = 280$ (number of FODO cells), $Q_x = 47.2$ and $Q_z = 47.2$ has been assumed. The response to a single plane wave depends sensitively on the direction of wave propagation with respect to the observation point. This dependence is not shown here.

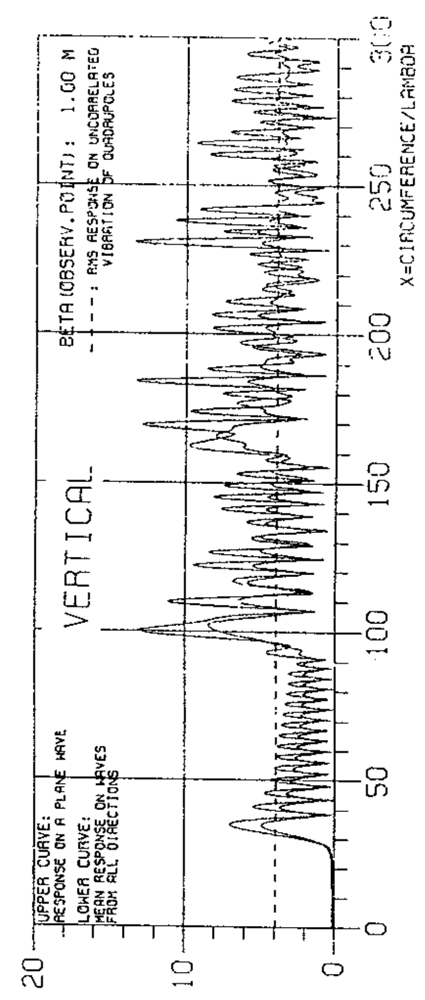

Fig. 29 Closed orbit response of a model periodic FODO lattice with parameter fitting the HERA proton ring: $N = 130$, $Q_x = 31.2$, $Q_z = 32.2$. As expected from the analytical model, the response becomes large for $C/\lambda = 30$, $130 - 30 = 100$, $130 + 30 = 160$, ... All resonances besides the first one are due to the FODO cell periodicity.

Fig. 30-36 Computer simulation of the actual HERA magnet lattices with respect to closed orbit response to a single ground wave. These results may be compared with results of analytical investigations, namely

figs. 30, 31 with fig. 28 (top)
fig. 32 with fig. 28 (bottom)
fig. 34 with fig. 29 (top)
fig. 35 with fig. 29 (bottom)

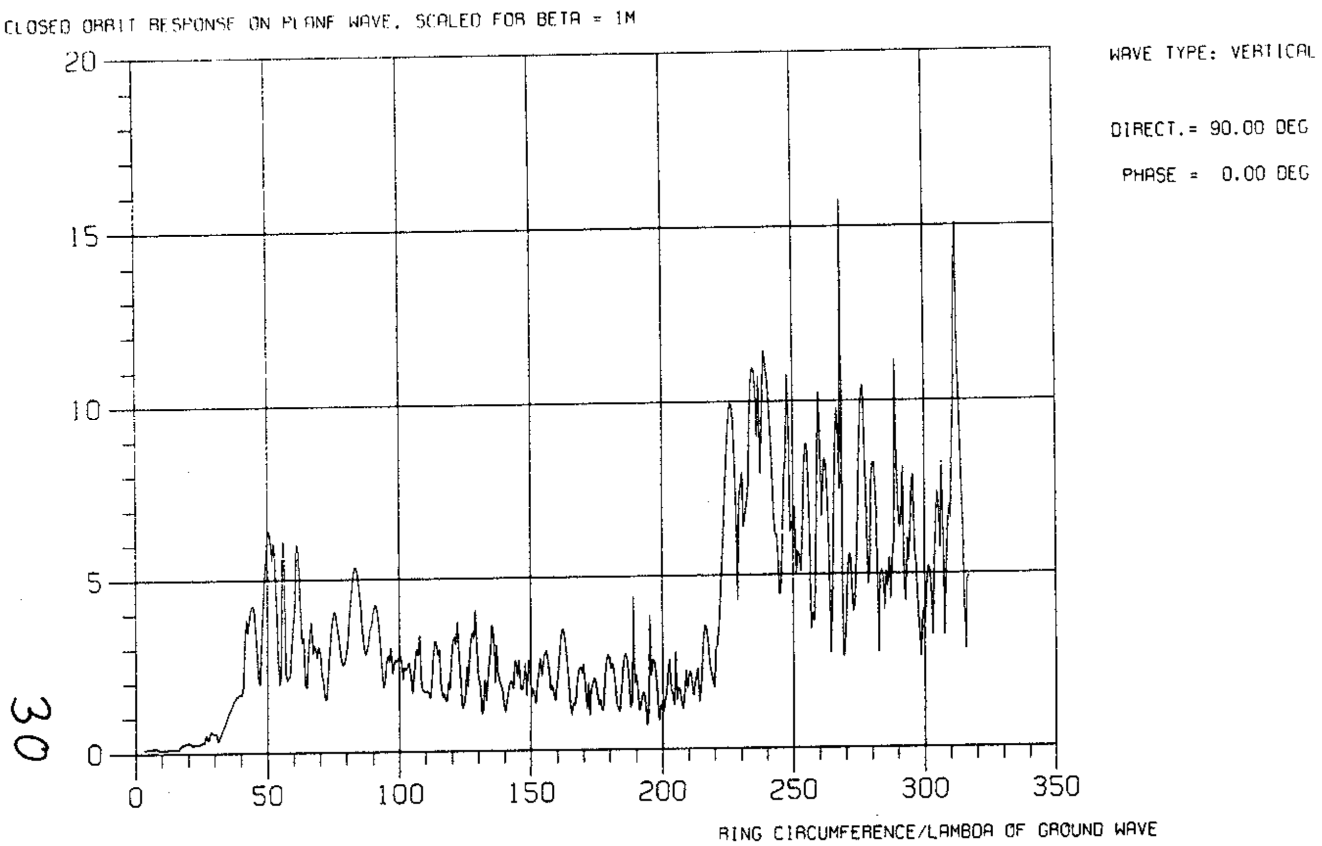

30

SPECTRAL RESPONSE OF HERA E('HE60Q3S6'); A=0.1MM, 550 STEPS

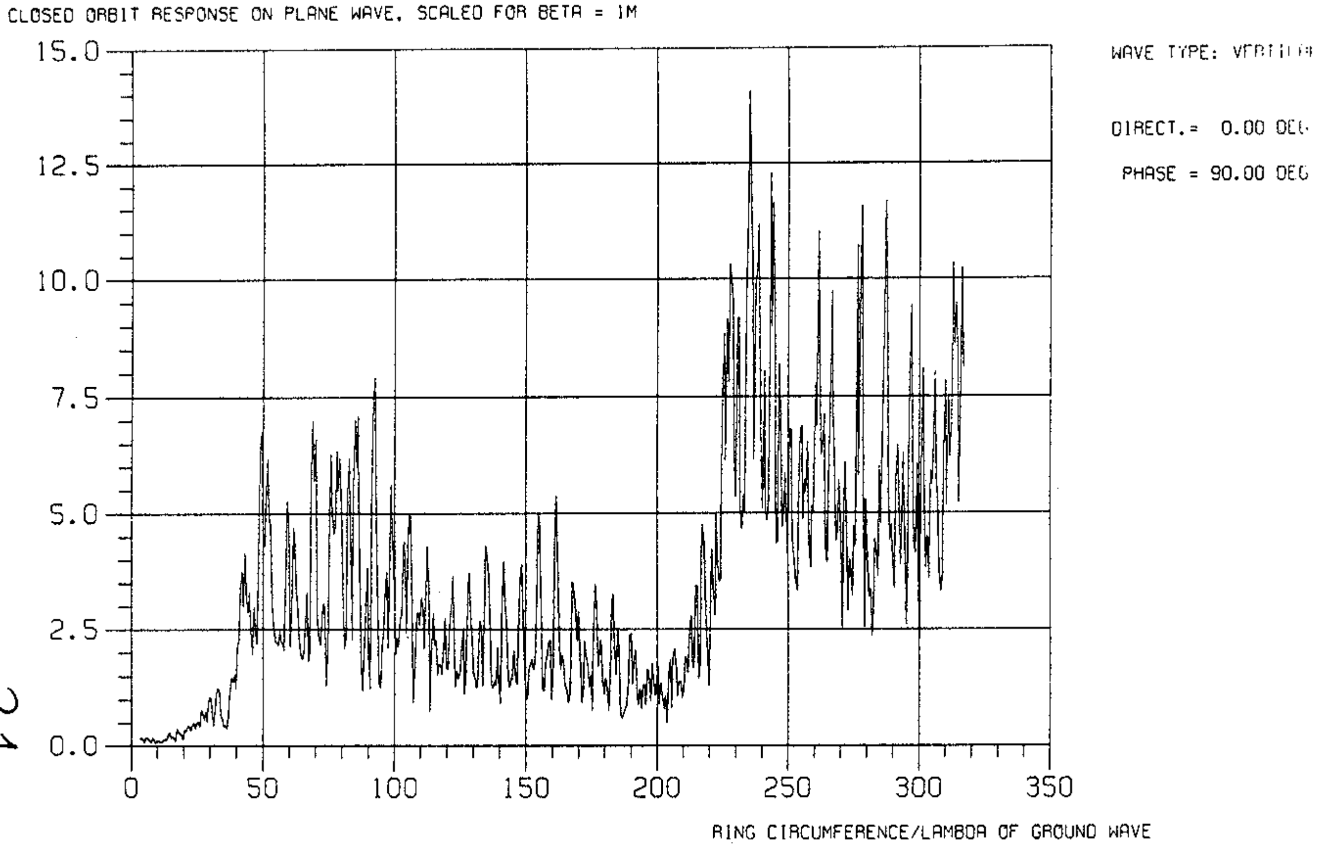

31

SPECTRAL RESPONSE OF HERA E; A=0.1MM, 550 STEPS

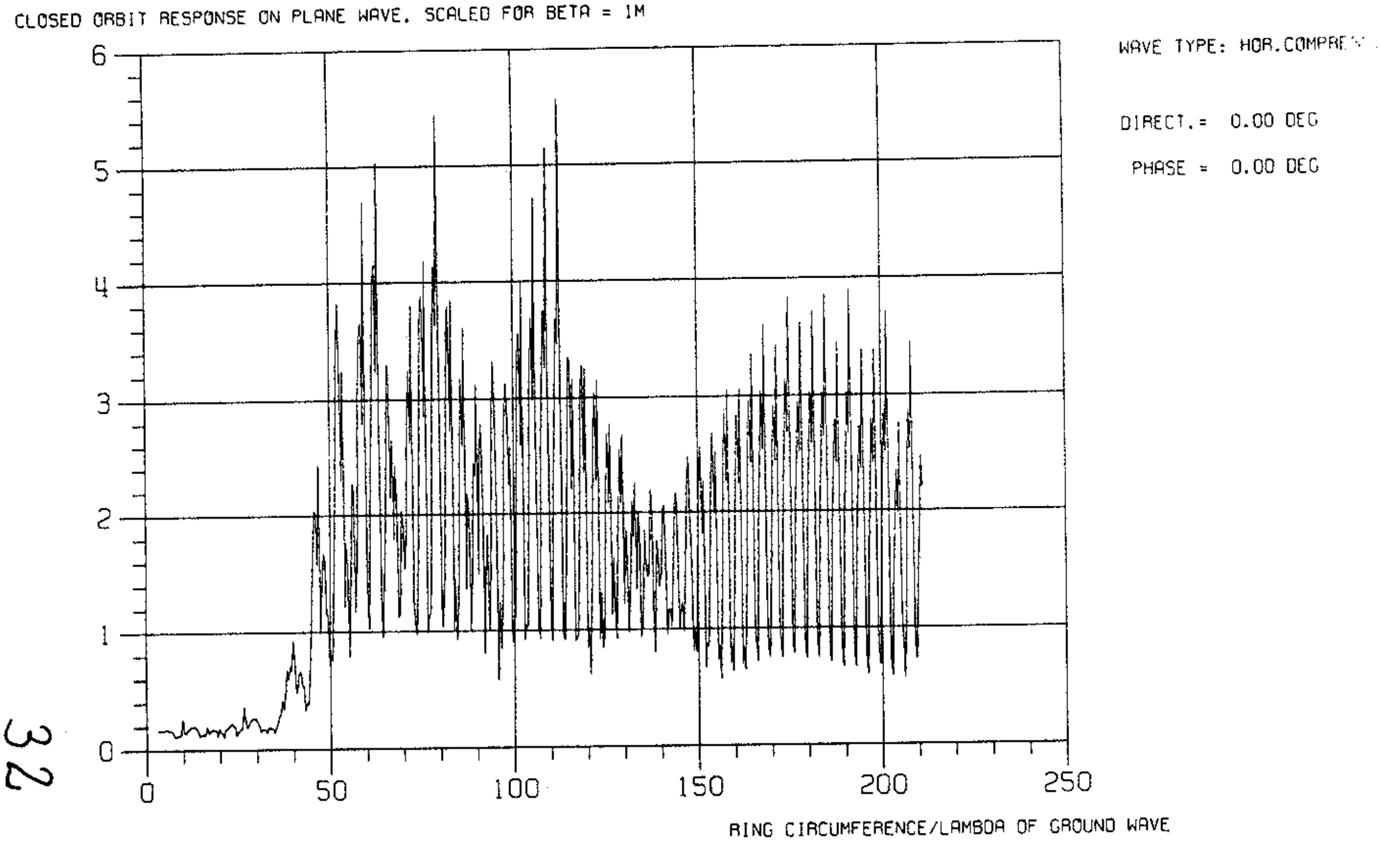

32

SPECTRAL RESPONSE OF HERA E; A=0.1MM, 500 STEPS

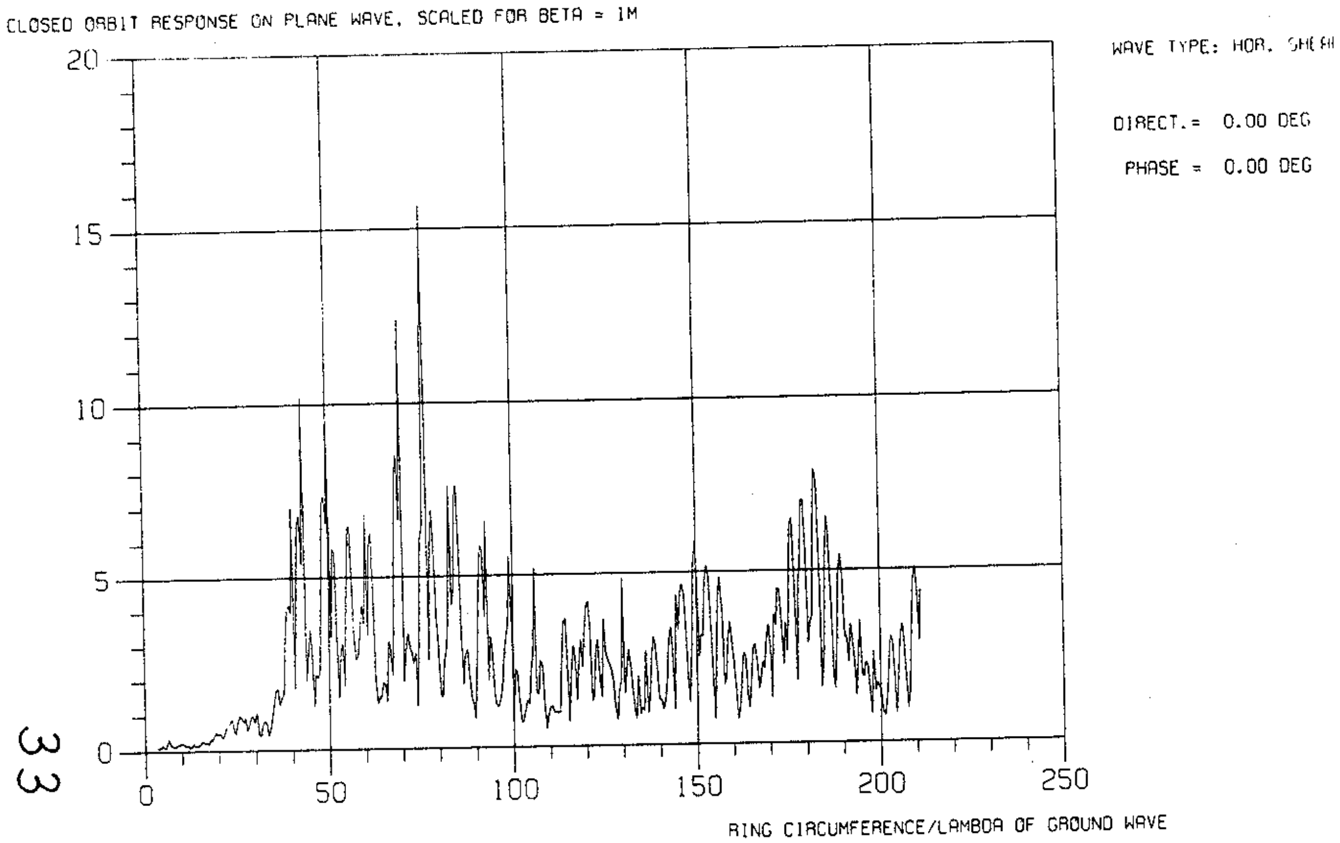

33

SPECTRAL RESPONSE OF HERA E: A=0.1MM, 400 STEPS

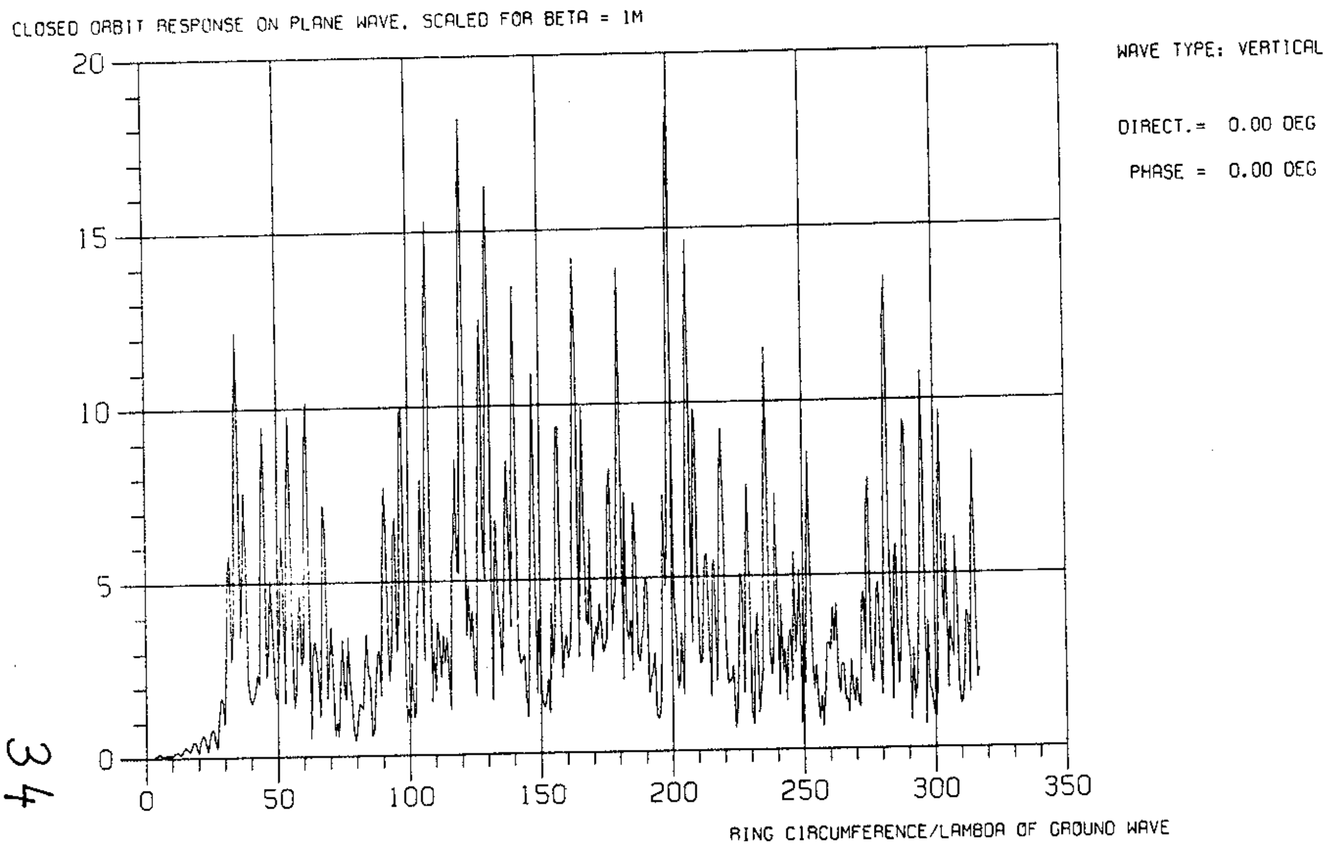

34

SPECTRAL RESPONSE OF HERA P('HPRINGL'): A=0.1MM, 450 STEPS

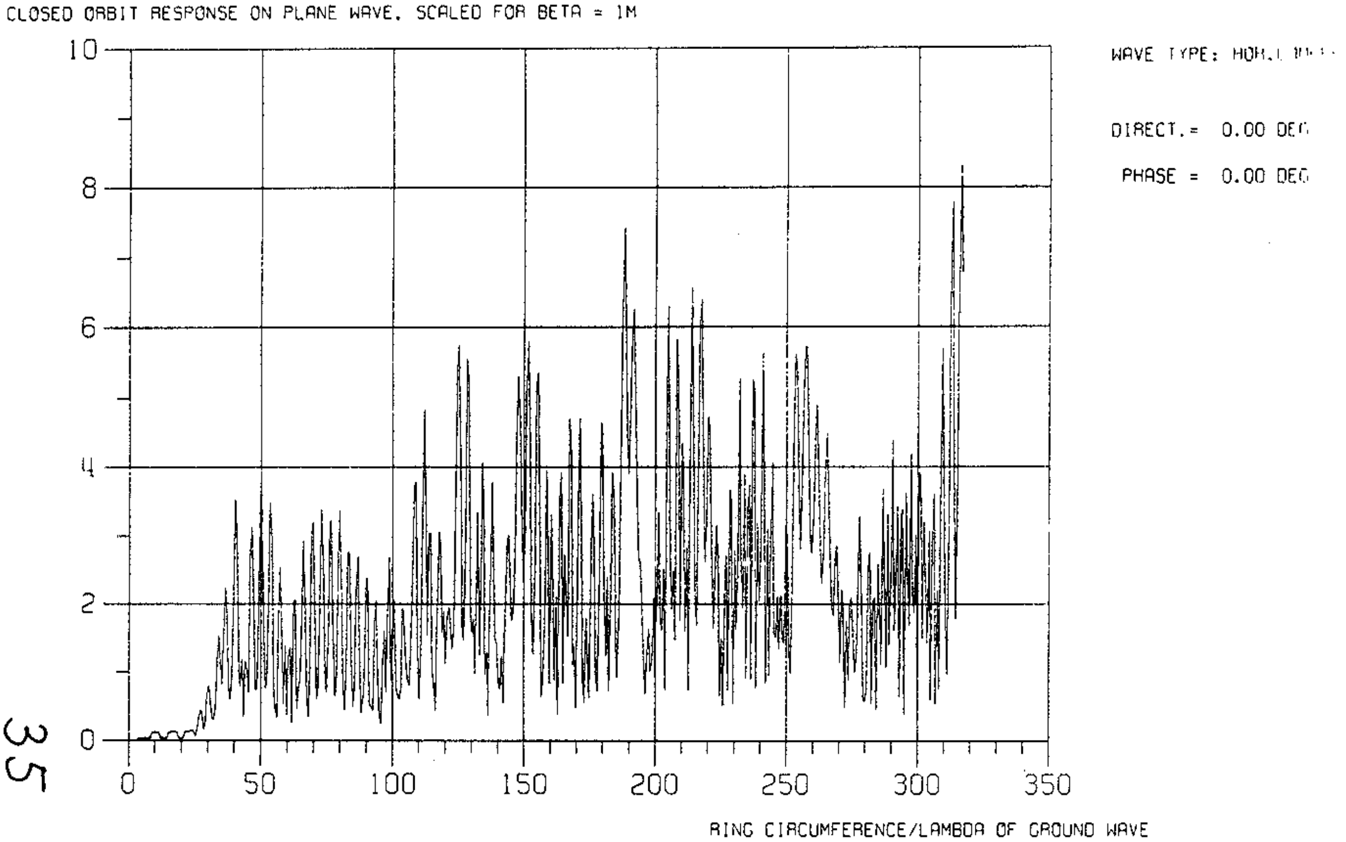

35

SPECTRAL RESPONSE OF HERA P('HPRINGL'); A=0.1MM, 500 STEPS

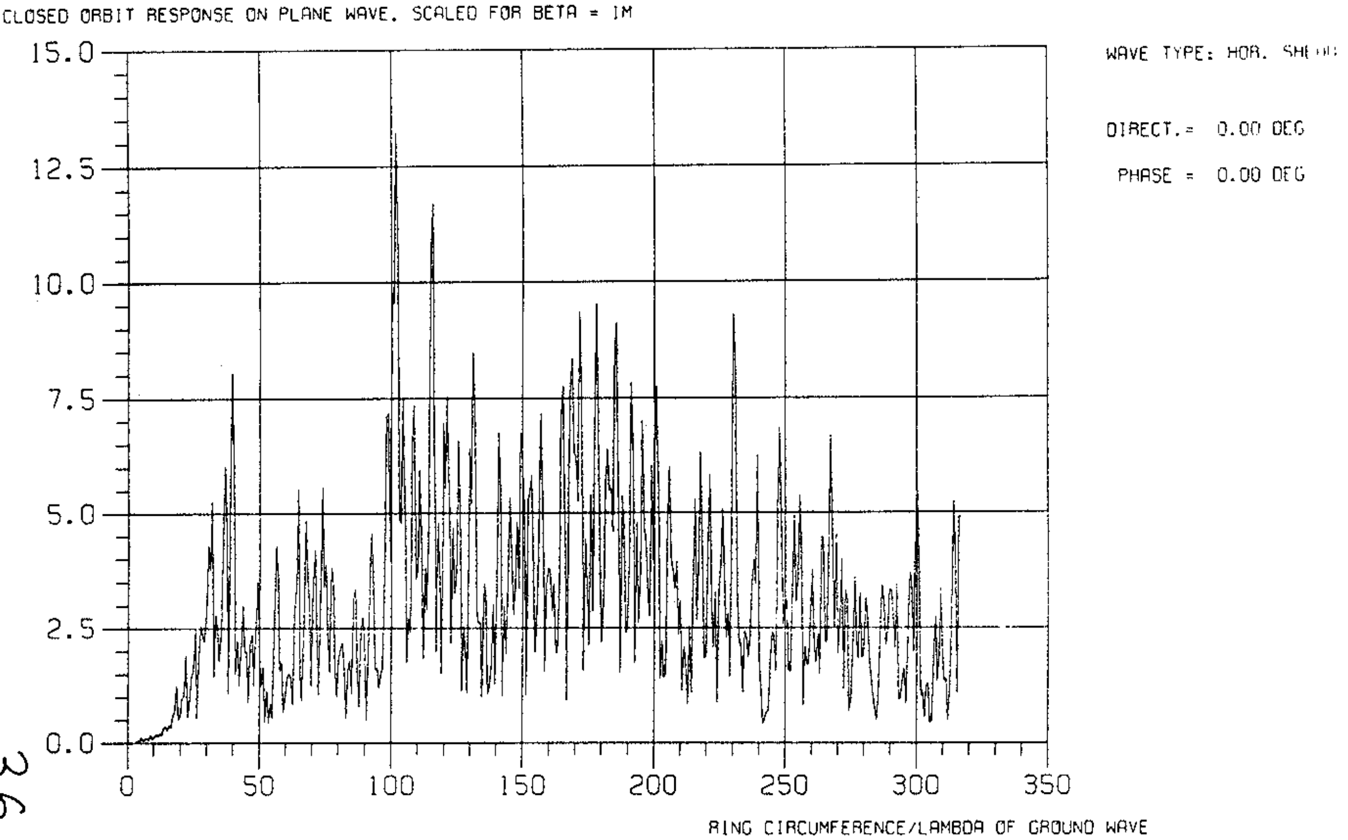

36

SPECTRAL RESPONSE OF HERA P('HPRINGL'); A=0.1MM, 450 STEPS